WELL-POSEDNESS AND STABILITY OF PLANAR CONEWISE LINEAR SYSTEMS

A THESIS SUBMITTED TO

THE GRADUATE SCHOOL OF ENGINEERING AND SCIENCE

OF BILKENT UNIVERSITY

IN PARTIAL FULFILLMENT OF THE REQUIREMENTS FOR

THE DEGREE OF

MASTER OF SCIENCE

IN

ELECTRICAL AND ELECTRONICS ENGINEERING

By

Daniyal Namdar

September, 2021

Well-Posedness and Stability of Planar Conewise Linear Systems
By Daniyal Namdar
September, 2021

We certify that we have read this thesis and that in our opinion it is fully adequate, in scope and in quality, as a thesis for the degree of Master of Science.

Prof. Dr. Arif Bülent Özgüler(Advisor)

Prof. Dr. Ömer Morgül

Assist. Prof. Dr. Aykut Yıldız

Approved for the Graduate School of Engineering and Science:

Ezhan Karaşan
Director of the Graduate School

ABSTRACT

WELL-POSEDNESS AND STABILITY OF PLANAR CONEWISE LINEAR SYSTEMS

Daniyal Namdar
M.S. in Electrical and Electronics Engineering
Advisor: Prof. Dr. Arif Bülent Özgüler
September, 2021

Planar conewise linear systems constitute a subset of piecewise linear systems. The state space of a conewise linear system is a finite number of convex polyhedral cones filling up the space. Each cone is generated by a positive linear combination of a finite set of vectors, not all zero. In each cone the dynamics is that of a linear system and any pair of neighboring cones share the same dynamics at the common border, which is itself a cone of one lower dimension. Each cone with its linear dynamics is called a mode of the conewise system.

This thesis focuses on the simplest case of planar systems that is composed of a finite number of cones of dimension two; with borders that are cones of dimension one, that is rays. Stability of such conewise linear systems is well understood and there are a number of necessary and sufficient conditions. Somewhat surprisingly, their well-posedness is not so well understood or studied except for the special case where there are two modes only, i.e, the bimodal case.

A graphical necessary and sufficient condition is here derived for the well-posedness of a planar conewise linear system of arbitrary number of modes and the well-known condition for stability is re-stated on this same graph. This graphical result is expected to provide some guidance to well-posedness studies of conewise systems in a higher dimension.

Keywords: Piecewise linear systems, Planar conewise linear systems, Well-posedness, Stability.

ÖZET

DÜZLEMDE-KONİK DORUSAL SİSTEMLERİN İYİ-TANIIMLILIĞI VE KARARLILIĞI

Daniyal Namdar
Elektrik ve Elektronik Mühendisliıgi, Yüksek Lisans
Tez Danışmanı: Prof. Dr. Arif Bülent Özgüler
Eylül, 2021

Konik doğrusal sistemler parçalı-doğrusal sistemlerin bir alt kümesidir. Konik doğrusal bir sistemin durum-uzayı, uzayıdolduran sonlu sayıda konveks polyhedral konilerden oluşur. Her bir koni sonlu sayıda, hepsi birden sıfır olmayan, sonlu sayıda vektörün pozitif doğrusal kombinasyonlarıyla elde edilir. Koni içindeki dinamik, bir doğrusal sistem dinamiğidir ve komşu olan her koni çifti, kendisi de bir alt boyutlu bir koni olan ortak sınırlarında aynıdinamiği paylaşırlar.

Bu tezde sonlu sayıda iki boyutlu konilerden oluşan en basit duruma, düzlemde-konik sistemlere odaklanılmaktadır. Bu özel durumda sınırlar da bir boyutlu konilerden, yani ışınlardan oluşmaktadır. Bu türden konik sistemlerin kararlılığıiyi anlaşılmıştır ve kararlılık için bir kaç adet değişik gerek ve yeter koşullar mevcuttur. İki boyutlu konink sistemlerin iyi-tanımlılığı ise, şaşırtçı bir şekilde, iki alt-sistemden ibaret özel durum haricinde, tam olarak incelenip anlaşılmamıştır.

Burada, sonlu sayıda alt-sistemlerden oluşan düzlemde-konik doğrusal bir systemin iyi-tanımlılığıiçin grafik kaideli bir gerek ve yeter koşul verilmekte ve literatürde iyi bilinen bir kararlılık sonucu da aynıgrafik üzerinde yeniden dile getirilmektedir. Bu grafik kaideli sonucun daha büyük boyutlu konik sitemlerin iyi-tanımlılığı için yol göstermesi beklenebilir.

Anahtar sözcükler: Parçalıdoğrusal sistemler, Konik doğrusal sistemler, iyi-tanımlılığıiçin, İIstikrar.

Acknowledgement

First and foremost, I would like to express my gratitude to Professor A. Bülent Özgüler, for his motivation and help throughout my Master's studies at Bilkent University. His insightful ideas and remarks considerably increased the quality of my research. I appreciate his assistance in teaching me how to conduct field research.

Apart from my advisor, I would like to show my sincere appreciation to Prof. Dr. Ömer Morgül and Dr. Aykut Yıldız, members of my thesis committee, for their time, encouragement, insightful comments, and challenging questions.

For anyone who has contributed indirectly to my thesis, I want to express a few remarks. My initial gratitude goes to friends who are always around every time I need them. Mahsa, Alireza, Soheil, and Ali. They have made my experience more pleasurable in Turkey and have helped me achieve my spiritual and academic goals. I am indebted to my wonderful colleague Muhammad Zakwan for his technical and moral support and our discussions about the research challenge, particularly during my first year. It is critical to strike a balance with life outside of the office. As a result, I can't emphasize enough how important my weekly retreat is, where I get to hang out with my friends who have been through this long process with me, always offering support and love.

Finally, I owe a debt of gratitude to my family: my father for inspiring me to pursue higher education outside of my home country, my mother for always being there for me and reminding me that I am awesome even when I didn't believe it, and my brother for his spiritual support through my most tough situation. I dedicate this work to my family because of their absolute, unequivocal, and loving support.

This work is supported by the Scientific and Technological Research Council of Turkey (TUBITAK) under project 116E229.

To my parents

Contents

List of Figures

Chapter 1

Introduction

A hybrid control system with continuous and discontinuous dynamic activity has gained a lot of interest in control system design because it has many practical control applications that blend continuous-time dynamics and switching characteristics. Hybrid systems may be found in various situations, including manufacturing, communication networks, autopilot design, and automobile engine management. Hybrid systems are essential in embedded control systems that interact with the physical environment [1],[2] .

As a result, several mathematical models and analytical techniques have been developed. The rudimentary class of hybrid control systems includes some of the simplest hybrid systems, such as piecewise affine (PWA) and piecewise linear (PWL) systems [3], [4]. PWL system study is necessary as a first step in creating hybrid control theory since PWL systems are one of the fundamental types of hybrid dynamical systems. This hybrid system is described by a state-space partition, which divides it into multiple regions with linear subsystems, each active in a distinct state-space region [5], [6]. Conewise piecewise linear systems are dynamical systems in which the state space is partitioned into a finite number of convex polyhedral cones, each of which is described by a linear differential equation [7], [8] [9], [10], and [11].

Despite their apparent simplicity in modeling, the stability analysis of conewise linear systems is complicated due to their hybrid nature, especially in the presence of sliding modes. Furthermore, it is difficult to apply controllability, observability, and well-posedness conclusions obtained from linear time-invariant systems to the situation of piecewise linear systems. The most accessible approach is to use a standard Lyapunov function to solve the problem [12], [13], [14], [15], and [16].

Finding a Lyapunov function for our piecewise linear systems, on the other hand, is a difficult task. In recent years, new approaches have been presented, such as [17], in which the author attempts to exploit switching transitions and introduce a transition graph approach for autonomous stability analysis. We can also observe in [18] that the stability of planar piecewise linear systems has been derived using a novel set of necessary and sufficient criteria based on a geometric approach. This innovative trajectory-based method is based on how the eigenvectors of a subsystem stand relative to the vectors that define the polyhedral cone.

Physical systems frequently function in several modes, transitioning from one mode to the next is idealized as an instantaneous, discrete change. Electrical circuits containing switching devices such as (ideal) diodes and transistors and mechanical systems subject to inequality constraints, such as those used in robotics, are examples. The well-posedness (existence and uniqueness of solutions) of the resulting hybrid system and the ability to efficiently simulate the multi-modal physical system are the primary concerns. The integrator dynamics give a basic example of a hybrid system that does not have unique solutions, at least from a particular point of view

$$\dot{y} = u$$

along with the relay element

$$\begin{aligned} u &= +1, \quad y > 0 \\ u &= -1, \quad y < 0 \\ -1 \leq u &\leq 1, \quad y = 0. \end{aligned}$$

It is clear that with the starting condition y(0) = 0, the system can develop in any of these three locations, resulting in the following solutions (i) y(t) = t, u(t) = 1, (ii) y(t) = -t, u(t) = -1, and (iii) y(t) = 0, u(t) = 0. As a result, we have three solutions beginning with the zero initial condition.

There are several sorts of phenomena in hybrid systems, such as multiple solutions, sliding motions, Zeno trajectories, and multiple events via jump solution. Hence, the well-posedness problem is critical in the development of hybrid systems [19].

1.1 Literature Review

Because hybrid systems provide an extensive modeling framework, there are no clearly verifiable necessary and sufficient requirements for generalized hybrid dynamical systems' well-posedness. It is already interesting to provide adequate requirements for the well-posedness of specific kinds of hybrid systems, such as piecewise affine systems (PWA), piecewise linear systems (PWL), linear relay systems, conewise linear systems (CLS), and so on. In this part, we give a summary of the paper devoted to the well-posedness problem of various hybrid systems.

We have a special subclass of PWL systems that only have two subsystems. Bimodal Piecewise Linear Systems and Bimodal Piecewise Affine Systems are named after homogeneous subsystems and a constant vector added to the vector field, respectively. In [20], the author investigates the well-posedness problem in terms of Carathéodory solutions with discontinuous vector fields for Bimodal Piecewise Linear Systems with observable modes. As necessary and sufficient requirements for well-posedness, a set of algebraic conditions and sign inequalities is presented. These criteria generate a joint structure for the system matrices of the two modes, and well-posedness conditions for bimodal piecewise affine systems reduce to well-posedness conditions for bimodal piecewise linear systems for certain system triples matrix configurations.

The framework of Linear Complementarity Systems (LCS) in [21] provides sufficient criteria for the uniqueness of the solution. In addition, several forms of uniqueness for LCS have been provided in [22], such as weakly uniqueness, right-zeno uniqueness, and the theorem for weak and local well-posedness derived from solution uniqueness. They offer global existence results for bimodal LCS in the last chapter.

The primary objective of the [23] is to explore the existence, uniqueness, and nature of solutions (as defined by Carathéodory and Filippov) for a specific class of piecewise affine dynamical systems, specifically bimodal piecewise affine systems with no external inputs. First, the authors demonstrates that the standard criteria used in the context of generic differential inclusions to ensure Filippov's uniqueness are somewhat restrictive in the context of piecewise affine systems. Then, for bimodal piecewise affine systems, they propose a set of necessary and sufficient criteria that assure the uniqueness of Filippov solutions. They offer criteria that rule out the so-called Zeno behavior (possibility of infinitely many switchings within a finite time interval) by examining the connections between Carathéodory and Filippov under the provided conditions.
This work is extended in [24] to multi-modal piecewise affine systems with external inputs and proposed a novel transition rule called the switch-based transition rule to explain the solution concept of a class of multi-modal hybrid systems with independent binary switches. When a part of vector fields is switched by binary switches, each of which works independently under autonomous switching, then this type of system is known as a switch-driven PWA system. The well-posedness of its subsystems of lower complexity bimodal systems is then derived as a sufficient condition for such a multi-modal system to be well-posed for all external inputs, which is algebraically and explicitly checkable and allows us to determine the well-posedness of the multi-modal systems in question algebraically.

This study [25] looks at a specific form of hybrid dynamics that occurs in linear dynamical systems with ideal relay components. Three modes of operation demonstrate the behavior of an ideal relay; hence, the uniqueness of solutions is not guaranteed. Based on the definition of a relay system as a complementarity system, they have demonstrated that if the transfer matrix is a P-matrix, then the relay system has a unique solution that is continuous in the state, therefore establishing the system's discrete transition rules.

As previously stated, one of the key difficulties in PWL systems is the problem of the existence and uniqueness of solutions in [26] the necessary and sufficient criteria for bimodal PWL discontinuous systems have been obtained from being well-posed under Carathéodory's notion of solutions. Also given is an extension to bimodal PWL discontinuous systems with multiple criteria. Finally, they talked about the multi-modal example with multiple criteria for the observable case. The conclusions are based on the lexicographic inequality relation and the smooth continuation feature.

The results of [26] were generalized to piecewise-linear systems with multiple modes and numerous criteria in [27]. They develop necessary and sufficient conditions for the well-posedness issue of piecewise-linear systems with multiple modes and multiple criteria without restricting themselves to the observable case exclusively. They also define mode well-posedness as the existence of a solution in a single mode. Article provided novel algorithmic techniques based on the well-known Fourier–Motzkin elimination methodology to test these criteria. A verifiable condition for the well-posedness of planar Conewise linear system has been derived in [28] under the assumption that there are no sliding modes. The condition is in terms of ta relationship among the entries of the state matrices of the modes, which is similar to the "flow continuity condition" in [29] also used for a characterization of well-posedness of planar conewise systems. An attempt has been made in [30] to generalize the well-posedness result of [30] to three-dimensions. The subspaces obtained from subsystem matrices are used to express the necessary and sufficient conditions for 3D CLS well-posedness.

1.1.1 Main Focus

Some recent research on CLS stabilization, such as [6] and [18], presume that the system is well-posed. The research [18] has provided a unique geometric condition for well-posedness under the assumption that there are no sliding mode. In [28], a well-posedness theorem for CLS based on various system matrices' entries and eigenvalues is obtained again under the assumption of no sliding modes. The generalization of this work in (3D) situations was explored in [31].

A uniform approach that allows sliding modes and all possible Jordan forms for the system matrices is clearly needed even in the simplest case of planar conewise systems.

Such an approach is adopted here and combined with a graph representation. There are thus two contributions of this thesis: 1) The condition of Imura and van der Schaft [26] for well-posedness of bimodal systems in terms of modal observability matrices is shown to apply also to two adjacent planar modes of a conewise system without any change. It has also been shown in Theorem 3.2.1 that this fact applies even when sliding modes are allowed. 2) A special graphical model of the conewise system is shown to be instrumental in unifying the check for well-posedness and stability of a planar CLS.

1.2 Outline

The following is the structure of this thesis. The mathematical model of conewise linear systems under focus is introduced in Chapter 2, along with a study of the trajectories. Some fundamental definitions and theorems from graph theory are also given in Chapter 2. The main results on well-posedness are discussed in Chapter 3. First, we determine a simple necessary and sufficient condition for the well-posedness of two adjacent modes in a planar conewise linear system. The condition is in terms of the eigenvectors and the generating vectors of the cones on which subsystems are defined. Then, using an associated graph, we state necessary and sufficient conditions for a multi-modal planar conewise linear system to be well-posed. Stability results of [6] and [18] are then re-phrased and stated on the same well-posedness graph.

1.3 Notation

We denote the real numbers, n-dimensional real vector space, and the set of real $n \times m$ matrices by $\mathbb{R}$, $\mathbb{R}^n$, and $\mathbb{R}^{n\times m}$, respectively. The norm of a vector $\mathbf{v} \in \mathbb{R}^n$ will be denoted by $|\mathbf{v}|$. The natural basis vectors in $\mathbb{R}^n$ will be denoted by $\mathbf{e}_i$, i=1, ...,n. In particular, when n = 3, we will use$\mathbf{k} := \mathbf{e}_3$. If $\mathbf{v}$,$\mathbf{w} \in \mathbb{R}^3$, then $\mathbf{v} \times \mathbf{w}$ will denote the cross product of the vectors and $\mathbf{v} \cdot \mathbf{w} = \mathbf{v}^T\mathbf{w}$, their dot product, where 'T' denotes 'transpose.' If $\mathbf{v}$,$\mathbf{w} \in \mathbb{R}^2$, then by $\mathbf{v} \times \mathbf{w}$, we mean det$[\mathbf{v} \;\; \mathbf{w}]\mathbf{k}$, where 'det' means' determinant,' i.e., cross product of vectors in the plane will be computed by imbedding them in the space. The set of complex n-vectors will be $\mathbb{C}^n$ and $j \in \mathbb{C}$ will be the imaginary number. For convenience, we will use the cross product of$\mathbf{v}$,$\mathbf{w} \in \mathbb{C}^2$ as well and define $\mathbf{v} \times \mathbf{w} :=$ det$[\mathbf{v} \;\; \mathbf{w}]\mathbf{k}$. By log z, z $\in \mathbb{C}$, we denote the complex principal logarithm log z = ln $|z| + j\angle z$ with $-\pi < \angle z < \pi$.

Chapter 2

Preliminaries

In this chapter, we will first outline the types of systems that we will be studying. The trajectories of a single-mode system are then investigated in Section 2.2. A system is classified as a sink, source, transitive, or half-sink in Section 2.3. Finally, in Section 2.4, certain definitions and facts from graph theory are presented.

2.1 Planar Conewise Linear Systems

The class of systems considered are

$$\dot{\mathbf{x}} = \begin{cases} A^1\mathbf{x} & if \quad \mathbf{x} \in \mathsf{S}^1, \\ A^2\mathbf{x} & if \quad \mathbf{x} \in \mathsf{S}^2, \\ \vdots & \vdots \quad \vdots \\ A^m\mathbf{x} & if \quad \mathbf{x} \in \mathsf{S}^m, \end{cases} \tag{2.1}$$

where $A^i \in \mathbb{R}^{2\times 2}$ and, with $C^i \in \mathbb{R}^{2\times 2}$,

$$\mathsf{S}^i := \{\mathbf{x} \in \mathbb{R}^2 : C^i\mathbf{x} \geq 0\},$$

for $i = 1, 2, ..., m$. We assume that each C^i is nonsingular and is such that $\det C^i > 0$. Note that the latter causes no loss of generality and only requires a permutation of rows of C^i if necessary. The nonsingularity assumption implies that each mode in (2.1) is active in a nonempty cone S^i, $int\,\mathsf{S}^i$ that is strictly contained in a half-space. We further assume that the interior of each pairwise intersection $int\,\mathsf{S}^i \cap \mathsf{S}^k$, $i \neq k$ is empty and that $\mathsf{S}^1 \cup ... \cup \mathsf{S}^m = \mathbb{R}^2$. Further, let

$$S^i = \begin{bmatrix} \mathbf{s}_1^i & \mathbf{s}_2^i \end{bmatrix} := (C^i)^{-1} = \begin{bmatrix} (\mathbf{c}_1^i)^T \\ (\mathbf{c}_2^i)^T \end{bmatrix}^{-1} \tag{2.2}$$

so that $\det S^i > 0$. Each S^i, $i = 1, ..., m$ is a convex polyhedral cone

$$\mathsf{S}^i = \{\alpha \mathbf{s}_1^i + \beta \mathbf{s}_2^i : \alpha, \beta \geq 0\},$$

and the boundary of S^i is the union two rays

$$\mathsf{B}_k^i = \{\alpha \mathbf{s}_k^i : \alpha \geq 0\}, \quad k = 1, 2.$$

It is easy to see that a vector $\mathbf{b} \in \mathsf{S}^i$ iff $\mathbf{c}_k^T \mathbf{b} \geq 0$ for $k = 1, 2$. Also note that because $\det S^i > 0$, the cross products $\mathbf{s}_1^i \times \mathbf{s}_2^i$ points upward using the right-hand rule, i.e., the two vectors are positively oriented. This allows us to label B_1^i and B_2^i as the right and left border, respectively.

By the nonsingularity assumption of each C^i and by the fact that the whole plane is covered by S^i's, it follows that the number of modes in (2.1) satisfies $m \geq 3$. Thus, the minimum number of modes must be three. This does not limit the class of conewise systems considered. A mode defined on a half-space or a sector larger than a half-space can be still covered by two modes defined on convex polyhedral cones of (2.1) having the same dynamics (the same A-matrix).

Given a mode i, its eigenvalues will be denoted by $\lambda_1^i, \lambda_2^i \in \mathbb{C}$ and, in case of real and distinct eigenvalues, they will be indexed so that $\lambda_1^i \geq \lambda_2^i$.

2.2 Single Mode Characterization

We now focus on a single mode i (and temporarily discard the index **i**) to consider

$$\dot{\mathbf{x}} = A\mathbf{x}, \quad \mathbf{x} \in \mathsf{S} \subset \mathbb{R}^2, \quad \mathsf{S} = \{\alpha \mathbf{s}_1 + \beta \mathbf{s}_2 : \alpha, \beta \geq 0\}, \tag{2.3}$$

where $\det S > 0$ for $S = [\mathbf{s}_1 \;\; \mathbf{s}_2]$. Let $\mathbf{v}_1, \mathbf{v}_2 \in \mathbb{R}^2$ be such that

$$AV = V\Lambda, \quad V = [\mathbf{v}_1 \;\; \mathbf{v}_2],$$

where Λ is one of

$$\Lambda_d := \begin{bmatrix} \lambda_1 & 0 \\ 0 & \lambda_2 \end{bmatrix}, \Lambda_r := \begin{bmatrix} \lambda & 1 \\ 0 & \lambda \end{bmatrix}, \Lambda_c := \begin{bmatrix} \sigma & \omega \\ -\omega & \sigma \end{bmatrix}, \Lambda_{sr} := \begin{bmatrix} \lambda & 0 \\ 0 & \lambda \end{bmatrix}, \tag{2.4}$$

respectively when the eigenvalues are such that $\lambda_1 > \lambda_2$ (real-distinct), $\lambda := \lambda_1 = \lambda_2$ (repeated), $\lambda_1 = \bar{\lambda}_2 = \sigma + j\omega$ (non-real) with $\omega > 0$, and $\lambda := \lambda_1 = \lambda_2$ (simple-repeated). It follows that if the eigenvalues are real-distinct, then $\mathbf{v}_1, \mathbf{v}_2$ are the eigenvectors associated with the larger and smaller eigenvalues, respectively. (With slight abuse of language, $\mathbf{v}_1, \mathbf{v}_2$ are the *larger and smaller eigenvectors*.) If the eigenvalues are repeated, then $\mathbf{v}_1$ is an eigenvector and $\mathbf{v}_2$ is a generalized eigenvector. If the eigenvalues are non-real, then $\mathbf{v}_1 + j\mathbf{v}_2$ is the eigenvector associated with $\sigma + j\omega$. Also in the simple-repeated case we have two linearly independent eigenvectors $\mathbf{v}_1$ and $\mathbf{v}_2$. Of course, in this case, every pair of linearly independent vectors will serve as valid eigenvectors. We will assume that whenever a mode defined on cone $S = [\mathbf{s}_1 \;\; \mathbf{s}_2]$ has simple-repeated eigenvalues, then its eigenvectors are chosen as $\mathbf{v}_1 = \mathbf{s}_1, \mathbf{v}_2 = \mathbf{s}_2$. We also define

$$W = \begin{bmatrix} \mathbf{w}_1^T \\ \mathbf{w}_2^T \end{bmatrix} := V^{-1}.$$

Note that, $\det V > 0$ if and only if $\mathbf{v}_1 \times \mathbf{v}_2$ is positively oriented.

The trajectory at $t \geq 0$ of (2.3) starting at $\mathbf{x}(0) = \mathbf{b} \in \mathsf{S}$ at time 0 can be written as

$$\mathbf{x}(t, \mathbf{b}) = \begin{cases} e^{\lambda_1 t}\mathbf{w}_1^T\mathbf{b}\mathbf{v}_1 + e^{\lambda_2 t}\mathbf{w}_2^T\mathbf{b}\mathbf{v}_2 \\ e^{\lambda t}\left[(\mathbf{w}_1^T\mathbf{b} + t\mathbf{w}_2^T\mathbf{b})\mathbf{v}_1 + \mathbf{w}_2^T\mathbf{b}\mathbf{v}_2\right] \\ e^{\sigma t}\left[(\mathbf{w}_1^T\mathbf{b}\cos(\omega t) + \mathbf{w}_2^T\mathbf{b}\sin(\omega t))\mathbf{v}_1 + (\mathbf{w}_2^T\mathbf{b}\cos(\omega t) - \mathbf{w}_1^T\mathbf{b}\sin(\omega t))\mathbf{v}_2\right] \\ e^{\lambda t}\mathbf{b} \end{cases} \tag{2.5}$$

for the four cases in (2.4), respectively. Examining the sign of the derivative of its angle, we can determine the direction the trajectory moves at any time. We note that in the simple-repeated case, the trajectory moves radially along the initial state $\mathbf{b}$. The other cases are now considered.

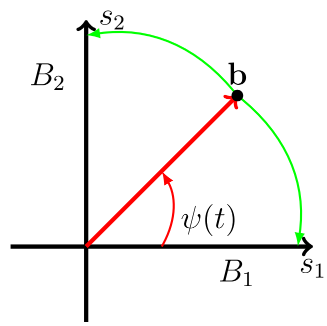

Figure 2.1: Trajectory direction

Fact 2.2.1 *Trajectory* $\mathbf{x}(t, \mathbf{b})$ *moves in a positive direction at time* $t \geq 0$ *if and only if*

$$\begin{cases} \det V\, \mathbf{w}_1^T \mathbf{b}\, \mathbf{w}_2^T \mathbf{b} < 0 & \textit{if eigenvalues are real-distinct,} \\ \mathbf{w}_2^T \mathbf{b} \neq 0, \det\, V < 0 & \textit{if eigenvalues are repeated,} \\ \det\, V < 0 & \textit{if eigenvalues are non-real,} \end{cases} \tag{2.6}$$

Proof. Let $\mathbf{x}(t, \mathbf{b}) = \rho(t) \angle \psi(t)$ be in polar representation. Then, $\tan \psi(t) = \mathbf{e}_2^T \mathbf{x} / \mathbf{e}_1^T \mathbf{x}$ so that

$$\dot{\psi}(t) = \frac{(\mathbf{e}_2^T \dot{\mathbf{x}})(\mathbf{e}_1^T \mathbf{x}) - (\mathbf{e}_1^T \dot{\mathbf{x}})(\mathbf{e}_2^T \mathbf{x})}{\rho^2}.$$

Computing the numerator via the appropriate expressions from (2.5), it is straightforward to obtain

$$\dot{\psi}(t) = \begin{cases} -\frac{\det V (\lambda_1 - \lambda_2)(\mathbf{w}_1^T \mathbf{b})(\mathbf{w}_2^T \mathbf{b})}{\rho^2 e^{-(\lambda_1 + \lambda_2)t}} & \text{if eigenvalues are real-distinct,} \\ -\frac{\det\, V (\mathbf{w}_2^T \mathbf{b})^2}{\rho^2 e^{-2\lambda t}} & \text{if eigenvalues are repeated,} \\ -\frac{\det\, V \omega [(\mathbf{w}_1^T \mathbf{b})^2 + (\mathbf{w}_2^T \mathbf{b})^2]}{\rho^2 e^{-2\sigma t}} & \text{if eigenvalues are non-real,} \end{cases}$$

which imply (2.6). □

We observe that, as long as the initial state does not lie along an eigendirection, the trajectory direction is independent of time and that, for the cases in which the eigenvalues are non-real or repeated, the direction is determined by the sign of $\det V$ only. In case of real-distinct eigenvalues, how the initial state is situated with respect to the two eigenvectors also matters. For instance, if $\det V > 0$ then the trajectory moves in the negative direction if and only if $(\mathbf{w}_1^T \mathbf{b})(\mathbf{w}_2^T \mathbf{b}) > 0$. This geometrically translates into the vector $\mathbf{b}$ being in between the two eigenvectors $\mathbf{v}_1$ and $\mathbf{v}_2$.

The following Lemma will elaborate on this fact and its relation with $\mathbf{c}_1^T\dot{\mathbf{x}}(t_1, \mathbf{b})$ which also determines the direction of the trajectory.

Lemma 2.2.1 *In the case of simple-repeated eigenvalues the trajectory* $\mathbf{x}(t, \mathbf{b})$ *remains inside the cone moving along the direction of* $\mathbf{b}\ \forall\ t \geq 0$.

The following Lemma relates the trajectory direction with $\mathbf{c}_k^T\dot{\mathbf{x}}(0, \mathbf{b})$, $k = 1, 2$.

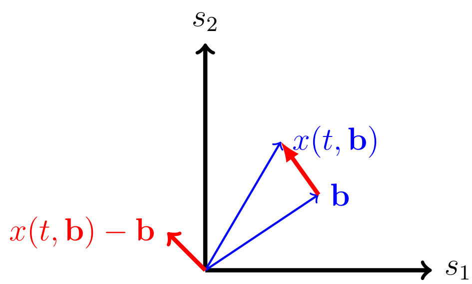

Figure 2.2: Positive direction trajectory related to $\mathbf{c}_k^T\dot{\mathbf{x}}(0, \mathbf{b})$

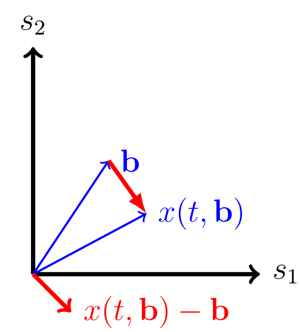

Figure 2.3: Negative direction trajectory related to $\mathbf{c}_k^T\dot{\mathbf{x}}(0, \mathbf{b})$

Lemma 2.2.2 *Let* $\mathbf{b} \in \mathsf{S}$. *The trajectory* $\mathbf{x}(t, \mathbf{b})$ *moves in the negative direction if and only if* $\mathbf{c}_2^T\dot{\mathbf{x}}(t, \mathbf{b}) < 0$. *The trajectory* $\mathbf{x}(t, \mathbf{b})$ *moves in the positive direction if and only if* $\mathbf{c}_1^T\dot{\mathbf{x}}(t, \mathbf{b}) < 0$. *The trajectory* $\mathbf{x}(t, \mathbf{b})$ *moves radially along* $\mathbf{b}$ *if and only if* $\mathbf{c}^T\dot{\mathbf{x}}(t, \mathbf{b}) = 0$ *for some vector* $\mathbf{c}$ *orthogonal to* $\mathbf{b}$, *i.e.,* $\mathbf{c}^T\mathbf{b} = 0$.

Proof. We examine the direction at $t = 0$ for simplicity as the same argument holds for any $t \geq 0$. Observe that $\mathbf{c}_2^T(\mathbf{x}(t, \mathbf{b}) - \mathbf{b}) < 0$ iff the trajectory moves towards B_1. We then have

$$\mathbf{c}_2^T\dot{\mathbf{x}}(t, \mathbf{b}) \mid_{t=0} = \lim_{t \to 0} \frac{\mathbf{c}_2^T\mathbf{x}(t, \mathbf{b}) - \mathbf{c}_2^T\mathbf{x}(0, \mathbf{b})}{t} = \lim_{t \to 0} \frac{\mathbf{c}_2^T\mathbf{x}(t, \mathbf{b}) - \mathbf{c}_2^T\mathbf{b}}{t} \tag{2.7}$$

and $\mathbf{c}_2^T\dot{\mathbf{x}}(0, \mathbf{b}) < 0$ iff the trajectory moves towards B_1. The second statement follows by the observation that $\mathbf{c}_1^T(\mathbf{x}(t, \mathbf{b}) - \mathbf{b}) < 0$ iff the trajectory moves towards B_2 and follows an analogous reasoning. $\square$

We can now examine the cases of trajectories hitting a boundary. Let us define for $k, i = 1, 2$

$$n_{ki}(\mathbf{b}) := \mathbf{c}_k^T\mathbf{v}_i\mathbf{w}_i^T\mathbf{b}$$

Fact 2.2.2 *Let* $\mathbf{b}$ *be strictly inside* S. *(i) There exists a finite* $t_1 > 0$ *such that* $\mathbf{x}(t_1, \mathbf{b})$ *intersects* B_1 *and goes out of the cone if and only if*

$$\begin{cases} n_{21}(\mathbf{b}) < 0 \;\&\; n_{21}(\mathbf{s}_1) < 0 & \textit{if eigenvalues are real-distinct,} \\ \det V > 0 \;\&\; \mathbf{c}_2^T \mathbf{v}_1\, \mathbf{w}_2^T \mathbf{b} < 0 & \textit{if eigenvalues are repeated,} \\ \det V > 0 & \textit{if eigenvalues are non-real.} \end{cases} \tag{2.8}$$

(ii) There exists a finite $t_2 > 0$ *such that* $\mathbf{x}(t_2, \mathbf{b})$ *intersects* B_2 *and goes out of the cone if and only if*

$$\begin{cases} n_{11}(\mathbf{b}) < 0 \;\&\; n_{11}(\mathbf{s}_2) < 0 & \textit{if eigenvalues are real-distinct,} \\ \det V < 0 \;\&\; \mathbf{c}_1^T \mathbf{v}_1\, \mathbf{w}_2^T \mathbf{b} < 0 & \textit{if eigenvalues are repeated,} \\ \det V < 0 & \textit{if eigenvalues are non-real.} \end{cases} \tag{2.9}$$

Proof. Since $\mathbf{b}$ is strictly inside S, we have that $\mathbf{c}_k^T \mathbf{b} > 0$ for $k = 1, 2$. (i) Suppose first that the eigenvalues are real-distinct. Such a $t_1 > 0$ exists just in case

$$\mathbf{c}_2^T \mathbf{x}(t_1, \mathbf{b}) = e^{\lambda_1 t_1} n_{21}(\mathbf{b}) + e^{\lambda_2 t_1} n_{22}(\mathbf{b}) = 0 \tag{2.10}$$

equivalently, just in case

$$t_1 = \frac{1}{\lambda_1 - \lambda_2} \ln\left(-\frac{n_{22}(\mathbf{b})}{n_{21}(\mathbf{b})}\right).$$

Note by the identity $n_{21}(\mathbf{b}) + n_{22}(\mathbf{b}) = \mathbf{c}_2^T \mathbf{b}$ that the ratio satisfies $-n_{22}(\mathbf{b})/n_{21}(\mathbf{b}) > 1$ iff $n_{21}(\mathbf{b}) < 0$ iff $t_1 > 0$. Hence, $n_{21}(\mathbf{b}) < 0$ is necessary and sufficient for the trajectory to hit B_1 in case of real-distinct eigenvalues. By Fact 2.2.1, the direction of the trajectory is negative (so that it is going out of the cone) if and only if $-\det V\, \mathbf{w}_1^T \mathbf{s}_1 \mathbf{w}_2^T \mathbf{s}_1 = n_{21}(\mathbf{s}_1) < 0$. Suppose, next, that the eigenvalues are repeated. Then, $t_1 > 0$ exists if and only if $\mathbf{c}_2^T \mathbf{x}(t_1, \mathbf{b}) = e^{\lambda t_1} \left[(\mathbf{c}_2^T \mathbf{v}_1)(\mathbf{w}_1^T \mathbf{b}) + t_1 (\mathbf{c}_2^T \mathbf{v}_1)(\mathbf{w}_2^T \mathbf{b}) + (\mathbf{c}_2^T \mathbf{v}_2)(\mathbf{w}_2^T \mathbf{b}) \right] = 0$, which holds just in case

$$n_{21}(\mathbf{b}) + n_{22}(\mathbf{b}) = \mathbf{c}_2^T \mathbf{b} = -t_1\, \mathbf{c}_2^T \mathbf{v}_1 \mathbf{w}_2^T \mathbf{b}.$$

It is clear from this equality that $t_1 > 0$ iff $\mathbf{c}_2^T \mathbf{v}_1 \mathbf{w}_2^T \mathbf{b} < 0$. By Fact 2..2.1, the direction of the trajectory is negative if and only if $\det V > 0$.

In the final case that eigenvalues are non-real, there exists such t_1 if and only if $\det \mathrm{V} > 0$, by (2.6) and by the fact that trajectories are always foci or centers. The expression for the hit time $t_1 > 0$ is obtained from (2.5) as

$$\tan(\omega t_1) = \frac{\mathbf{c}_2^T \mathbf{b}}{\mathbf{c}_2^T \mathbf{v}_2 \mathbf{w}_1^T \mathbf{b} - \mathbf{c}_2^T \mathbf{v}_1 \mathbf{w}_2^T \mathbf{b}}.$$

(ii) The proof is analogous to (i). □

2.3 Mode Types

For the planar conewise linear systems, we have five different types of modes based on trajectory behavior. Here, we give the definitions of the mode types in the 2D case for real and distinct eigenvalues. For a generalization of the 2D definitions given below to higher dimensions, the reader is referred to Definition 2.3.1 of [32].

Definition 2.3.1 *i) A mode* S *is a* **sink** *if for every* $\mathbf{b} \in \mathsf{S}$ *and for all* $t \geq 0$, $\mathbf{x}(t, \mathbf{b}) \in \mathsf{S}$.

ii) A mode is a **transitive** *from its border* B_k *if, (a) for every* $0 \neq \mathbf{b} \in \mathsf{S}$, *there exists a finite* $t_k^* > 0$ *such that* $\mathbf{x}(t_k^*, \mathbf{b}) \in \mathsf{B}_k$ *and* $\mathbf{x}(t, \mathbf{b}) \in \mathsf{S}$ *for all* $t \in (0, t_k^*)$ *and (b) for any* $\mathbf{b} \in \mathsf{B}_j$, $j \neq k$, *there is* $\epsilon > 0$ *such that* $\mathbf{x}(t, \mathbf{b}) \in \mathsf{S}$ *for all* $t \in (0, \epsilon)$.

iii) A mode is a **source** *if, first, for every* $0 \neq \mathbf{b} \in \mathsf{B}_k$, *there exists a finite* $\epsilon > 0$ *such that* $\mathbf{x}(t, \mathbf{b}) \notin \mathsf{S}$ *for all* $t \in (0, \epsilon]$ *and, second, for all* $\mathbf{b} \in \mathsf{S}$, *except those on a cone of dimension one, there exists* $t^* > 0$ *such that* $\mathbf{x}(t^*, \mathbf{b}) \in \mathsf{B}_k$ *and* $\mathbf{x}(t, \mathbf{b}) \in \mathsf{S}$.

iv) A mode is a **half-sink** *if it is not one of (i)-(iii)*

In the half-sink cases, the sector consists of two different sectors with different behavior in each. In the sector which has a characteristic like a sink, no trajectories that start in the mode will go out. In the transitive cases, trajectories come in from one border and move out of the cone from the other border without converging to the origin or diverging to infinity.

The trajectory that starts in a cone may converge to the origin or diverge to infinity but never go out of the cone in a sink. On the other hand, In a source, the trajectory that starts in the cone moves out of the cone into one of the neighbors, except those that start on a ray that extends from the origin to infinity inside the cone.

Definition 2.3.2 *: An eigenvector* $\mathbf{v}$ *is interior to* S *if* $\mathbf{v}$ *or* $-\mathbf{v}$ *is in int*(S)*; it is exterior to* S *if neither* $\mathbf{v}$ *nor* $-\mathbf{v}$ *is in* S*. For non-real eigenvalues, the eigenvectors are always exterior.*

Example 2.3.1 *For a better understanding of different mode types consider a system with four modes where the boundary vectors are:*

$$\mathbf{s}_1 = \begin{bmatrix} 1 \\ 0 \end{bmatrix}, \quad \mathbf{s}_2 = \begin{bmatrix} 0 \\ 1 \end{bmatrix}, \quad \mathbf{s}_3 = \begin{bmatrix} -1 \\ 0 \end{bmatrix}, \quad \mathbf{s}_4 = \begin{bmatrix} 0 \\ -1 \end{bmatrix}$$

we have six different modes which are in cone$\{\mathbf{s}_1, \mathbf{s}_2\}$*, cone*$\{\mathbf{s}_2, \mathbf{s}_3\}$*, cone*$\{\mathbf{s}_3, \mathbf{s}_4\}$*, and cone*$\{\mathbf{s}_1, \mathbf{s}_4\}$*.*
The state matrices for the CLS are given as:

$$A^1 = A^2 = \begin{bmatrix} 1.5 & 0.5 \\ 0.5 & 1.5 \end{bmatrix}, \quad A^3 = \begin{bmatrix} \frac{11}{6} & -\frac{2}{3} \\ \frac{2}{3} & \frac{1}{6} \end{bmatrix}, \quad A^4 = \begin{bmatrix} \frac{7}{3} & -\frac{2}{3} \\ \frac{2}{3} & \frac{2}{3} \end{bmatrix}, \quad A^5 = A^6 = \begin{bmatrix} \frac{2}{3} & \frac{2}{3} \\ -\frac{2}{3} & \frac{7}{3} \end{bmatrix}.$$

The eigenvalues for the A^1 *and* A^2 *are* $\lambda_1^1 = \lambda_2^1 = 2, \lambda_1^2 = \lambda_2^2 = 1$ *also for the mode 3 we have* $\lambda_1^3 = 1.5, \lambda_2^3 = 0.5$ *for the fourth mode the eigenvalues are* $\lambda_1^4 = 2, \lambda_2^4 = 1$ *finally for the last two modes the eigenvalues are* $\lambda_1^5 = 2, \lambda_2^5 = 1$ *and* $\lambda_1^6 = 2, \lambda_2^6 = 1$*. The eigenvectors for each mode are as below:*

$$V^1 = V^2 = \begin{bmatrix} 1 & -1 \\ 1 & 1 \end{bmatrix}, \quad V^3 = \begin{bmatrix} -1 & -0.5 \\ -0.5 & -1 \end{bmatrix},$$

$$V^4 = \begin{bmatrix} 1 & 0.5 \\ 0.5 & 1 \end{bmatrix}, \quad V^5 = \begin{bmatrix} 1 & -2 \\ 2 & -1 \end{bmatrix}, \quad V^6 = \begin{bmatrix} -1 & 2 \\ -2 & 1 \end{bmatrix}.$$

Figure 2.4 thus illustrates that the eigenvector positions relative to the cone as well as to each other completely characterize the mode types in 2D cases.

1. *A mode with the smaller eigenvector interior to its cone and the other exterior is a source.*

2. *A mode with the larger eigenvector interior to its cone and the other exterior is a sink.*

3. *A mode with both eigenvector exterior to its cone is transitive. The direction of transitivity is further determined by the relative positions of the two eigenvectors among themselves.*

4. *A mode with both eigenvectors interior to its cone is a half-sink. The transitive sector is differentiated from the sink sector again by how the two eigenvectors stand with respect to each other.*

Figure 2.5 illustrates the mode types in the case of negatively oriented eigenvectors and real and distinct eigenvalues.

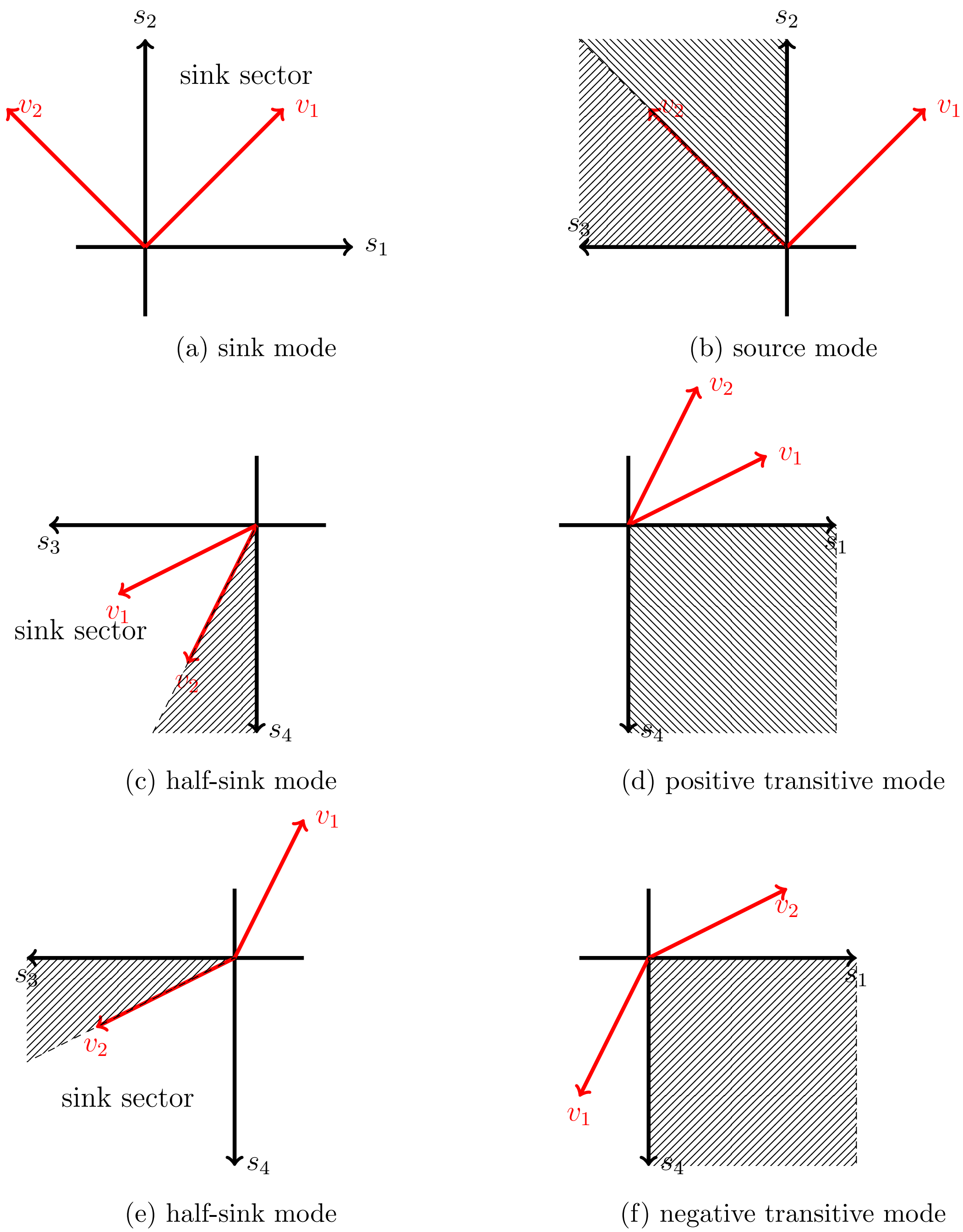

Figure 2.4: Positions of the eigenvectors relative to the cone with real and distinct eigenvalues for positively oriented case

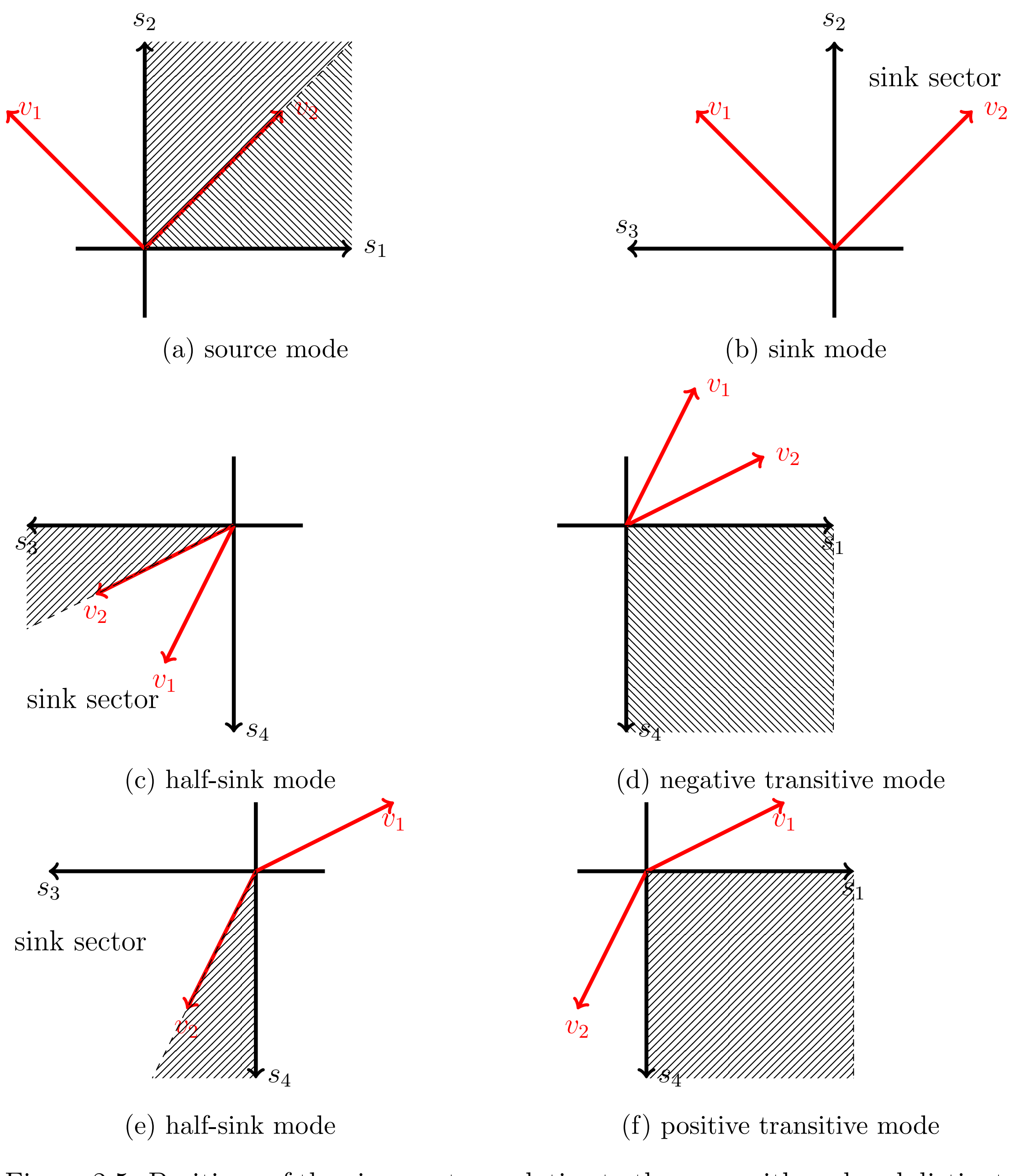

(a) source mode

(b) sink mode

(c) half-sink mode

(d) negative transitive mode

(e) half-sink mode

(f) positive transitive mode

Figure 2.5: Positions of the eigenvectors relative to the cone with real and distinct eigenvalues for negatively oriented case

We now consider the mode types for the case of real repeated eigenvalues. The possible mode types are then transitive, half-sink, and sink. The trajectory direction is clockwise when $\det \mathrm{V} > 0$ and counterclockwise when $\det \mathrm{V} < 0$. It is important to note that the position of $\mathbf{v}_2$ is relevant only as far as it determines the direction of trajectories via the sign of $\det \mathrm{V}$. The position of the larger eigenvector $\mathbf{v}_1$ settles the mode type.

For the third case of non-real eigenvalues, we only have the transitive type modes with $\det \mathrm{V}$ determining the direction of the trajectory. Trajectory moves in the clockwise direction for the positive determinant counterclockwise direction for the negative determinant. (Note that positively oriented eigenvectors correspond to a negative (clockwise) direction of trajectories as a consequence of Fact 2.2.1.)

Finally, for the simple repeated eigenvalue case, the trajectory always moves along the direction of the initial state. Moreover, the trajectories that start on the border will remain on the border irrespective of the choice of the eigenvectors.

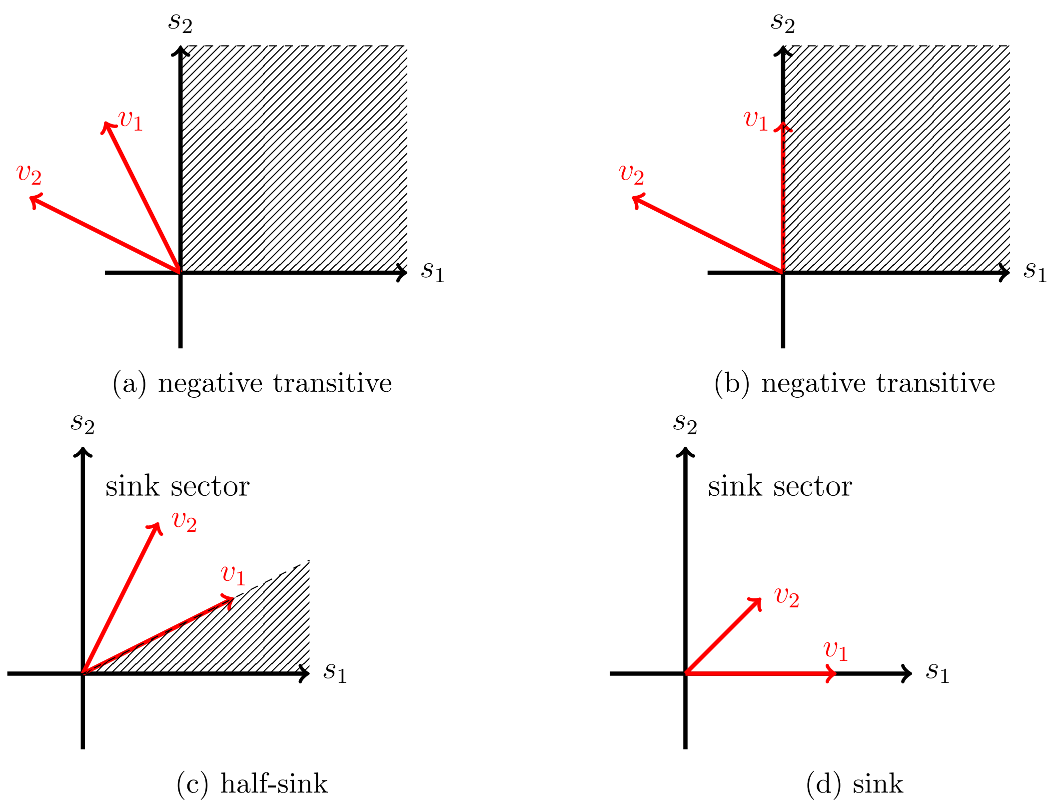

Figure 2.6: Positions of the eigenvectors relative to the cone $\{\mathbf{s}_1, \mathbf{s}_2\}$ for positively oriented real and repeated eigenvalues

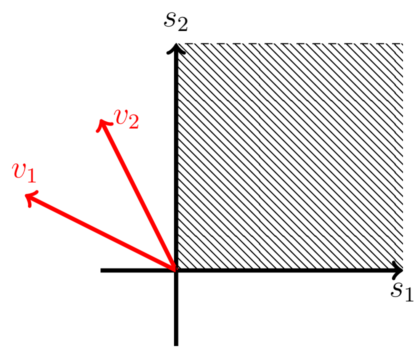

(a) positive transitive

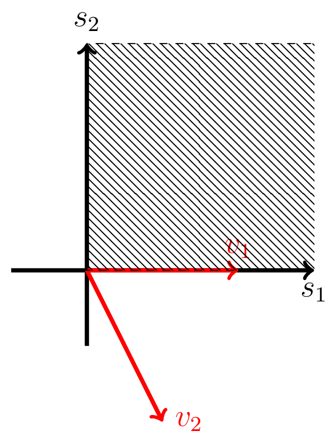

(b) positive transitive

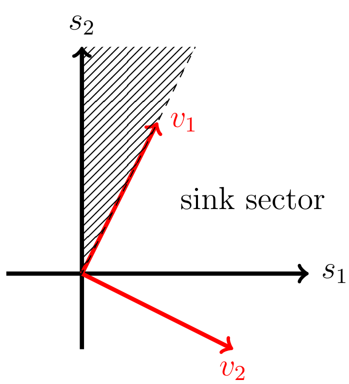

(c) half-sink

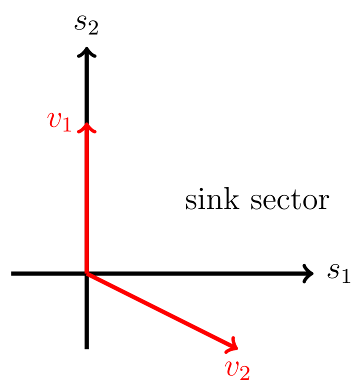

(d) sink

Figure 2.7: Positions of the eigenvectors relative to the cone $\{\mathbf{s}_1, \mathbf{s}_2\}$ for negatively oriented real and repeated eigenvalues

2.4 Directed Graphs

Graph theory is a study of the relationship between edges and vertices. A mathematical representation of a network and the relationship between edges and vertices are described in graphs. In this section, we focus on some definitions and elementary properties of directed graphs. The reader is referred to the books [33], [34], and [35] for more details of the definitions and results stated in this section.

A graph G consists of a finite nonempty set V of objects called vertices and a set E of 2-element subsets of V called edges. A **node** v is an intersection point of a graph. It denotes a location such as a town or in our case, a mode. An **edge** e is a link between two nodes. Which denotes the flow of the trajectory between the nodes. It has a direction that is generally represented as an arrow. If an arrow is not used, it means the link is bi-directional.

If e = uv is an edge of G, then the adjacent vertices u and v are said to be joined by the edge e. The vertices u and v are referred to as neighbors of each other. In this case, the vertex u and the edge e (as well as v and e) are said to be **incident** with each other. Distinct edges incident with a common vertex are adjacent edges.

If we proceed from u to a neighbor of u and then to a neighbor of that vertex and so on, until we finally come to a stop at a vertex v, then we have just described a **u-v walk** from u to v in G.

Definition 2.4.1 *A* ***digraph*** *(or directed graph) D is a finite nonempty set V of objects called vertices together with a set E of ordered pairs of distinct vertices. The elements of E are called directed edges or arcs. If (u, v) is a directed edge, then we indicate this in a diagram representing D by drawing a directed line segment or curve from u to v.*

Definition 2.4.2 *A u-v walk in a graph in which no vertices are repeated is a u-v* ***path****. A graph G is* ***connected*** *if every two vertices of G are connected, that* *is, if G contains a u-v path for every pair u, v of vertices of G.*

Definition 2.4.3 *The **degree** of a vertex v in a graph G is the number of edges incident with v and is denoted by* $deg_G\ v$ *or simply by deg v if the graph G is clear from the context. Also, deg v is the number of vertices adjacent to v.*

Definition 2.4.4 *When the vertices of graph G have the same degree then G is called **regular**. If degree of v is r for every vertex v of G, then G is **r-regular**.*

Definition 2.4.5 *A directed graph is **weakly connected** if the underlying graph of it is connected.*

Definition 2.4.6 *A directed graph D is **strongly connected** if, for every pair of vertices u and v in D, there exists a u-v path as well as a v-u path.*

(a) (b)

Figure 2.8: Graph representations of weakly ((a),(b)) and strongly connected (a) graphs.

(a) (b)

Figure 2.9: Examples of not connected graphs.

Definition 2.4.7 *Let G be a graph of order n and size m, where $V(G) = \{v_1, v_2, ..., v_n\}$ and $E(G) = \{e_1, e_2, ..., e_m\}$. The **adjacency matrix** of G is the $n \times n$ matrix $A = [a_{ij}]$, where*

$$a_{ij} = \begin{cases} 1 & if v_i v_j \in E(G) \\ 0 & otherwise \end{cases} \tag{2.11}$$

Example 2.4.1 *The adjacency matrix of the graphs in Definition 2.4.6 are as below*

$$A_a = \begin{bmatrix} 0 & 1 & 0 & 0 \\ 0 & 0 & 0 & 1 \\ 1 & 0 & 0 & 0 \\ 0 & 0 & 1 & 0 \end{bmatrix}, A_b = \begin{bmatrix} 0 & 1 & 0 & 0 \\ 0 & 0 & 0 & 1 \\ 0 & 0 & 0 & 0 \\ 0 & 0 & 1 & 0 \end{bmatrix}$$

Definition 2.4.8 *A directed walk is a directed **trail** if all its edges are distinct. A directed trail is open if its end vertices are distinct; otherwise it is closed*

Definition 2.4.9 *An open directed trail is a **directed path** if all its vertices are distinct. A closed directed trail is a **directed cycle** if all its vertices except the end vertices are distinct.*

Definition 2.4.10 *A graph with at least one directed cycle is known as a **directed cyclic** graph.*

Definition 2.4.11 *A directed graph is said to be **acyclic** if it has no directed cycle.*

See the directed graph in Figure 2.10 (a).

We may use the adjacency matrix to check the connectedness of its graph as follows [34].

(a) (b)

Figure 2.10: Examples of directed acyclic (a) and cyclic (b) graphs.

A digraph is disconnected if and only if its vertices can be sorted so that its adjacency matrix A can be represented as the direct sum of two square submatrices X_1 and X_2

$$A = \begin{bmatrix} X_1 & . & 0 \\ .. & . & .. \\ 0 & . & X_2 \end{bmatrix}. \tag{2.12}$$

This partitioning is only possible if and only if the vertices in the submatrix X_1 have no edges leading to or from the vertex of X_2. A digraph is similarly weakly connected if and only if its vertices can be sorted in such a way that its adjacency matrix can be written as

$$A = \begin{bmatrix} X_1 & . & 0 \\ .. & . & .. \\ X_{21} & . & X_2 \end{bmatrix} \tag{2.13}$$

or

$$A = \begin{bmatrix} X_1 & . & X_{12} \\ .. & . & .. \\ 0 & . & X_2 \end{bmatrix}, \tag{2.14}$$

where X_1 and X_2 denote square submatrices. When there is no edge connecting the subdigraph corresponding to X_1 to the one corresponding to X_2, the form 2.13 is used. When there is no edge connecting the subdigraph corresponding to X_2 to the subdigraph corresponding to X_1, the form 2.14 is used.

A digraph is strongly connected if and only if the vertices of A cannot be sorted in such a way that its adjacency matrix A is in the form 2.12, 2.13, or 2.14.

Lemma 2.4.1 *[36] The directed graph is acyclic if and only if its adjacency matrix is nilpotent.*

Proof. The matrix A^k counts the number of walks of length k in an adjacency matrix (recall that A is nilpotent if $A^k = 0$ for some $k \geq 1$). Generally the number of k-length walks from i to j is A^k_{ij}. which is multiply k factors of matrix A to raise it to the k-th power and considering the row i column j entry. If the A matrix is not nilpotent, then, for any $n \geq 1$, $A^n \neq 0$. Hence, there are n-length walks and there must be at least one cycle (because the same node must appear on the walk more than once if there are n edges in the walk). This gives that we have a cyclic directed graph. If A is nilpotent, on the other hand, we can permute its rows and columns at the same time to make it upper-triangular with zeros on the diagonal. Then, a cycle necessitates an edge from i to j but for $j < i$ all entries are zero so that no cycle exists, i.e., the graph must be acyclic. $\square$

Chapter 3

Well-posedness of Planar Linear Systems

The existence and uniqueness of solutions, referred to as well-posedness, is a rudimentary concern in studying hybrid systems [26]. Well-posedness problems have been considered in [37] for various subclasses hybrid systems such as multi-modal piecewise affine systems. In [26], necessary and sufficient conditions, primarily for bimodal piecewise linear systems, have been derived based on smooth continuation property of solution and using lexicographic inequalities.

In this chapter, we will first go over some basic concepts of well-posedness. In Section 3.2, two adjacent planar conewise linear systems are considered and a relevant result of [26] on bimodal systems is reviewed. In Section 3.3, a graph representation of multi-modal systems is described. The main graphical result on well-posedness of 2D conewise systems is then given in Section 3.4.

3.1 Well-posedness

Consider a first order vector differential equation together with an initial condition

$$\dot{\mathbf{x}}(t) = \mathbf{f}(t, \mathbf{x}(t)),\ \mathbf{x}(t_0) = \mathbf{b}.$$

Then, $\mathbf{x}(t)$ is a solution in the sense of Caratheodory for the initial state $\mathbf{b}$ in the interval $[t_0, t_1)$ if $\mathbf{x}(t)$ is absolutely continuous on $[t_0, t_1)$, satisfies the initial condition, and satisfies the differential equation almost everywhere in on $[t_0, t_1)$. Such a solution satisfies the following Caratheodory equation

$$\mathbf{x}(t) = \mathbf{b} + \int_{t_0}^{t_1} \mathbf{f}(\mathbf{x}(\tau))d\tau$$

and has a continuous derivative almost everywhere in $[t_0, t_1)$.

Definition 3.1.1 *Given the CLS (2.1),* $\mathbf{x}(t, \mathbf{b}), t \in [0, t_1)$ *is a solution of (2.1) if it is a solution on* $\in [0, t_1)$ *in the sense of Caratheodory, where the function* $\mathbf{f}(t, \mathbf{x}(t)) = \mathbf{f}(\mathbf{x}(t))$ *is given by the right hand side of (2.1).*

We now recall the definition of smooth continuation.

Definition 3.1.2 *[26]: The system (2.1) is said to be well-posed if for every initial state* $\mathbf{x}(0) = \mathbf{b} \in \mathbb{R}^2$*, there exists a unique forward Caratheodory solution* $\mathbf{x}(t, \mathbf{b}), t \geq 0$.

Definition 3.1.3 *[38]: Let* S *be a subset of* $\mathbb{R}^2$*. If for the initial state* $\mathbf{b}$ *there exists an* $\epsilon > 0$ *such that* $\mathbf{x}(t, \mathbf{b}) \in \mathsf{S}$ *for all* $t \in [0, \epsilon]$*, then we say that the system has the smooth continuation property at* $\mathbf{b}$ *with respect to* S*, or that smooth continuation is possible from* $\mathbf{b}$ *with respect to* S*. Moreover, if from all* $\mathbf{b} \in \mathsf{S}$ *smooth continuation is possible with respect to* S*, then the system is said to have the smooth continuation property with respect to* S*.*

Now we can now adopt the following result from Lemma 2.1 of [26] (see Remark 2.5 of [26]).

Lemma 3.1.1 *The following statements are equivalent.*
i) The system (2.1) is well-posed.
ii) For every initial state $\mathbf{b} \in \mathbb{R}^{\mathbf{2}}$ *of (2.1), smooth continuation is possible in only one of the two adjacent modes, i.e., if* i *and* k *are two adjacent modes, then smooth continuation is possible with respect to either* S^i *or* S^k*, except for the case that the solutions in both modes are the same in some time interval.*

Smooth continuation is possible even in the presence of, so called, "sliding modes."

Definition 3.1.4 *If a trajectory that starts at a border of a cone at* $x(0) = \mathbf{b}$ *remains in that border for all* $t \in [o, \epsilon)$ *for some* $\epsilon > 0$*, then it is called a sliding mode of the cone at that border.*

Note that in 2D, we have the following fact.

Fact 3.1.1 *There is a sliding mode at a border if and only if there is an eigenvector belonging to one of the adjacent modes on that border.*

Proof. If there is an eigenvector $\mathbf{v}$ at a border $\mathbf{s}$ of a mode and if an initial vector $\mathbf{b}$ is on that border, then $\mathbf{w}^T\mathbf{b} = 0$, for any orthogonal $\mathbf{w}$ to $\mathbf{v}$, It follows by the expressions (2.5) for solutions that the solution remains along the eigenvector $\mathbf{v}$, or equivalently along $\mathbf{s}$ for all $t > 0$, i.e., it is a sliding mode. Conversely, if there is an initial vector $\mathbf{b}$ on a border such that (2.5) $\mathbf{x}(t, \mathbf{b})$ remains at that border for an interval $t \in [0, \epsilon)$, then the trajectory moves radially in the direction of $\mathbf{s}$, or equivalently, in the direction of $\mathbf{b}$. By Lemma (2.2.2), $\mathbf{c}^T\mathbf{b} = 0$, for any orthogonal $\mathbf{c}$ to $\mathbf{b}$ as well $\mathbf{c}^T\mathbf{x}(t, \mathbf{b}) = 0$ for $t \in [0, \epsilon)$. The expression (2.5) now gives, in cases where an eigenvector $\mathbf{v}$ exists, that $\mathbf{c}^T\mathbf{v} = 0$, i.e., $\mathbf{v}$ is on the border. $\square$

3.2 Adjacent Modes

Let us consider two neighbor modes Mode-i and Mode-k with the common border $\mathsf{B}_2^i = \mathsf{B}_1^k$ defined by the vector $\mathbf{s}_2^i = \mathbf{s}_1^k$. (The left border for Mode-i is the right border for Mode-k.) It follows that $C^i = (S^i)^{-1}$ and $C^k = (S^k)^{-1}$ of (2.2) are such that $\mathbf{c}_2^i = \alpha\, \mathbf{c}_1^k$ for some $\alpha \in \mathbb{R}$. Let

$$V^i = \begin{bmatrix}\mathbf{v}_1^i & \mathbf{v}_2^i\end{bmatrix} = \begin{bmatrix}(\mathbf{w}_1^i)^T \\ (\mathbf{w}_2^i)^T\end{bmatrix}^{-1} = (W^i)^{-1}, \quad V^k = \begin{bmatrix}\mathbf{v}_1^k & \mathbf{v}_2^k\end{bmatrix} = \begin{bmatrix}(\mathbf{w}_1^k)^T \\ (\mathbf{w}_2^k)^T\end{bmatrix}^{-1} = (W^k)^{-1},$$

be the eigenvector matrices and their inverses so that

$$A^i = V^i \Lambda^i W^i, \quad A^k = V^k \Lambda^k W^k,$$

where Λ^i, Λ^k, are the Jordan forms that can be any one of (2.4) for either mode. Also recall that, for $h, k, i = 1, 2$, we have

$$n_{ki}^h(\mathbf{b}) := (\mathbf{c}_k^h)^T \mathbf{v}_i^h (\mathbf{w}_i^h)^T \mathbf{b} = (\mathbf{c}_k^h)^T A^h \mathbf{b}$$

for any vector $\mathbf{b}$.

Consider two matrices of observability

$$\mathcal{O}^i := \begin{bmatrix}(\mathbf{c}_2^i)^T \\ (\mathbf{c}_2^i)^T A^i\end{bmatrix}, \ \mathcal{O}^k := \begin{bmatrix}(\mathbf{c}_1^k)^T \\ (\mathbf{c}_1^k)^T A^k\end{bmatrix}.$$

Let, for $a \in \mathbf{R}$,

$$sign(a) := \begin{cases} 1 & a > 0 \\ -1 & a < 0 \\ 0 & a = 0 \end{cases}$$

Theorem 3.2.1 *Two adjacent modes Mode-i and Mode-k are well-posed if and only if one of the following equivalent conditions* **C1** *and* **C2** *holds:*

C1. *If neither Mode-i nor Mode-k has a sliding mode at* $\mathsf{B}_2^i = \mathsf{B}_1^k$*, then*

a. *either for both h=i and h=k,*

$$\begin{cases} sign\ \ n_{11}^h(s_2^i) < 0 & \textit{if eigenvalues are distinct,} \\ \det V^h < 0 & \textit{otherwise} \end{cases}$$

b. *or, both for h=i and h=k,*

$$\begin{cases} sign \;\; n_{11}^h(s_2^i) > 0 & \textit{if eigenvalues are distinct,} \\ \det V^h > 0 & \textit{otherwise.} \end{cases}$$

In case there is a sliding mode at $\mathsf{B}_2^i = \mathsf{B}_1^k$*, then there is a common eigenvalue of Mode-i and Mode-k, the corresponding eigenvectors of which have the same direction and both are at the common border.*

C2. *If the matrices* $\mathcal{O}^i$, $\mathcal{O}^k$ *are both nonsingular, then* $\mathcal{O}^i(\mathcal{O}^k)^{-1}$ *is lower triangular with positive diagonal entries. If one of* $\mathcal{O}^i$, $\mathcal{O}^k$ *is singular, then* $Ker\,\mathcal{O}^i = Ker\,\mathcal{O}^k$ *and for every* $\mathbf{b} \in Ker\,\mathcal{O}^i$*, it holds that* $A^i\mathbf{b} = A^k\mathbf{b}$.

Proof. Suppose **C1** holds and there is no sliding sliding mode at the common border. If **a** holds and h=i, then by Fact 2.2.2 part (ii) with $\mathbf{b} = s_2^i$, we get $n_{11}^i(s_2^i) < 0$ and $\det V^i < 0$ for the real and distinct eigenvalues and real-repeated or non-real eigenvalues. This gives that the trajectory moves in a positive direction and crosses the boundary B_2^i. If h=k, then $n_{11}^k(s_2^i) < 0$ and $\det V^k < 0$ for the real and distinct eigenvalues and real-repeated or non-real eigenvalues, respectively. Again by Fact 2.2.2 part (i) with $b = s_2^i$, the trajectory travels in a positive direction at the boundary B_1^k. It follows that if **C1**, **a** holds then the trajectories smoothly continue from Mode-i to Mode-k as required by Lemma 3.1.1 for well-posedness. Similarly, using Fact 2.2.2, if **C1**, **b** holds, then the trajectories smoothly continue from Mode-k to Mode-i.

Conversely, suppose that there is no sliding mode and that the two modes are well-posed. Then, by Lemma 3.1.1, the trajectories in both modes smoothly continues and at the common border, the trajectories either continue from Mode-i to Mode-k, i.e., in a positive direction, or from Mode-k to Mode-i, i.e., in a negative direction. Consider Fact 2.2.2 and initial condition $\mathbf{b} = s_2^i$. The trajectory will move in a positive direction in Mode-i if and only if $n_{11}^i(s_2^i) < 0$, and $\det V^i < 0$ for the real and distinct eigenvalues and real-repeated or non-real eigenvalues. This gives that **C1**, **a** holds. Similarly, considering Fact 2.2.2 and initial condition $\mathbf{b} = s_1^k$, the trajectory will move in a positive direction in Mode-k if and only if $n_{11}^k(s_1^k) < 0$, and $\det V^k < 0$ for the real and distinct eigenvalues and real-repeated or non-real eigenvalues. This gives that **C1**, **a** holds. Now consider again Fact 2.2.2 and initial condition $\mathbf{b} = s_2^i$. The trajectory will move in a negative direction in Mode-i if and only if $n_{11}^i(s_2^i) > 0$, and $\det V^i > 0$ for the real and distinct eigenvalues and real-repeated or non-real eigenvalues. This gives that **C1**, **b** holds.

Suppose now that there is a sliding mode at the common border. If **C1** holds, then there is a common eigenvalue, say $\lambda := \lambda^i = \lambda^k$, the eigenvectors v^i and v^k of which satisfy $v^i = \alpha v^k$ for a positive α. Every initial value $\mathbf{b}$ at the common border can then be written as $\mathbf{b} = \beta v^i = \beta\alpha v^k$ for some real number β such that $\mathbf{b} \in cone\{s_2^i\}$. Then, solutions in both modes have the expression $\mathbf{x}(t, \mathbf{b}) = e^{\lambda t}\mathbf{b}$, i.e., they are the same in both modes. Conversely, suppose that the solutions that start at an initial value $\mathbf{b} \in cone\{s_2^i\}$ are the same in both modes. Since we assumed that there is a sliding mode, there is an eigenvector of one mode, say $v^i \in cone\{s_2^i\}$ with eigenvalue λ^i. The solution in Mode-i that starts at the common border has then the expression $\mathbf{x}(t, \mathbf{b}) = e^{\lambda^i t}\mathbf{b}$. For smooth continuation, Mode-k must have the same solution. This gives that one eigenvalue of Mode-i must satisfy $\lambda^i = \lambda^k$ and its corresponding eigenvector v^i must also satisfy $v^i = \alpha v^k$ for a positive α.

Consider **C2** and suppose the eigenvalues of both modes are distinct. Multiplying observability matrices on the right by S^i, we have

$$\mathcal{O}^i S^i = \begin{bmatrix} \alpha & 0 \\ \star & \alpha(\lambda_1^i - \lambda_2^i)\,(\mathbf{c}_1^k)^T\,\mathbf{v}_1^i(\mathbf{w}_1^i)^T\,\mathbf{s}_2^i \end{bmatrix},\ \mathcal{O}^k S^i = \begin{bmatrix} 1 & 0 \\ \star & (\lambda_1^k - \lambda_2^k)(\mathbf{c}_1^k)^T\mathbf{v}_1^k(\mathbf{w}_1^k)^T\,\mathbf{s}_2^i \end{bmatrix},$$

so that (with '$\star$' meaning not needed)

$$\mathcal{O}^i(\mathcal{O}^k)^{-1} = \begin{bmatrix} \alpha & 0 \\ \star & \beta \end{bmatrix},\beta := \alpha\frac{\lambda_1^i - \lambda_2^i}{\lambda_1^k - \lambda_2^k}\frac{(\mathbf{c}_1^k)^T\,\mathbf{v}_1^i(\mathbf{w}_1^i)^T\,\mathbf{s}_2^i}{(\mathbf{c}_1^k)^T\,\mathbf{v}_1^k(\mathbf{w}_1^k)^T\,\mathbf{s}_2^i}. \tag{3.1}$$

(It is easy to see that nonsingularity of $\mathcal{O}^i$ is equivalent to "no sliding modes at B_2^i" for Mode-i, which in turn is equivalent to no (true) eigenvector being along $\mathbf{s}_2^i$.) It follows that **C2** holds iff α, β are positive, which in turn is the case, iff $(\mathbf{c}_1^k)^T\,\mathbf{v}_1^i(\mathbf{w}_1^i)^T\,\mathbf{s}_2^i$ and $(\mathbf{c}_1^k)^T\mathbf{v}_1^k(\mathbf{w}_1^k)^T\,\mathbf{s}_2^i$ have the same sign, in view of $\lambda_1^i > \lambda_2^i$, $\lambda_1^k > \lambda_2^k$. This establishes the equivalence of **C1** and **C2** in the case of distinct eigenvalues in both modes, because

$$(\mathbf{c}_1^k)^T \mathbf{v}_1^i (\mathbf{w}_1^i)^T \mathbf{s}_2^i = n_{11}^i(\mathbf{s}_2^i), and$$
$$(\mathbf{c}_1^k)^T \mathbf{v}_1^k (\mathbf{w}_1^k)^T \mathbf{s}_2^i = n_{11}^k(\mathbf{s}_2^i)$$

For the real and repeated case we have the same observability matrices with different eigenvector Jordan form which results in

$$\mathcal{O}^i S^i = \begin{bmatrix} \alpha & 0 \\ \star & \alpha\, \lambda^i\, (\mathbf{c}_1^i)^T\, \mathbf{s}_2^i + \alpha (\mathbf{c}_1^i)^T \mathbf{v}_1^i (\mathbf{w}_2^i)^T\, \mathbf{s}_2^i \end{bmatrix},$$
$$\mathcal{O}^k S^i = \begin{bmatrix} 1 & 0 \\ \star & \lambda^k\, (\mathbf{c}_1^k)^T\, \mathbf{s}_2^i + (\mathbf{c}_1^k)^T \mathbf{v}_1^k (\mathbf{w}_2^k)^T\, \mathbf{s}_2^i \end{bmatrix},$$

then we have

$$\mathcal{O}^i (\mathcal{O}^k)^{-1} = \begin{bmatrix} \alpha & 0 \\ \star & \beta \end{bmatrix}, \beta := \alpha \frac{\lambda^i\, (\mathbf{c}_1^k)^T\, \mathbf{s}_2^i + \det\, V^i ((\mathbf{w}_2^i)^T\, \mathbf{s}_2^i)^2}{\lambda^k\, (\mathbf{c}_1^k)^T\, \mathbf{s}_2^i + \det\, V^k ((\mathbf{w}_2^k)^T\, \mathbf{s}_2^i)^2}. \tag{3.2}$$

In the same way, we get the following matrices when we have non-real eigenvalues

$$\mathcal{O}^i (\mathcal{O}^k)^{-1} = \begin{bmatrix} \alpha & 0 \\ \star & \beta \end{bmatrix}, \beta := \alpha \frac{\sigma^i\, (\mathbf{c}_1^k)^T\, \mathbf{s}_2^i + \omega^i\, \det\, V^i \left[((\mathbf{w}_1^i)^T\, \mathbf{s}_2^i)^2 + ((\mathbf{w}_2^i)^T\, \mathbf{s}_2^i)^2 \right]}{\sigma^k\, (\mathbf{c}_1^k)^T\, \mathbf{s}_2^i + \omega^k\, \det\, V^k \left[((\mathbf{w}_1^k)^T\, \mathbf{s}_2^i)^2 + ((\mathbf{w}_2^k)^T\, \mathbf{s}_2^i)^2 \right]}. \tag{3.3}$$

As a consequence, **C2** holds iff α, β are positive, which in turn is the case, iff $\det\, V^i$, and $\det\, V^k$ both have the same sign. Now, it is easy to see that, **C1.a** holds iff the trajectories move from Mode-i to Mode-k and **C1.b** holds iff the trajectories move from Mode-k to Mode-i. Now suppose that there is a sliding mode at the common border. If **C2** holds then the following matrices are singular

$$\mathcal{O}^i S^i = \begin{bmatrix} \alpha & 0 \\ \star & (\mathbf{c}_2^i)^T A^i \mathbf{s}_2^i \end{bmatrix},$$

$$\mathcal{O}^k S^i = \begin{bmatrix} 1 & 0 \\ \star & (\mathbf{c}_1^k)^T A^k \mathbf{s}_2^i \end{bmatrix},$$

so, we need to have $(\mathbf{c}_2^i)^T A^i \mathbf{s}_2^i = (\mathbf{c}_1^k)^T A^k \mathbf{s}_2^i = 0$. This is the same as both modes have an eigenvector on the shared border from **C1**. Moreover, with an initial

$b = s_2^i$ we have the following solution:

$$A^i s_2^i = e^{\lambda_1^i t} s_2^i, \quad \text{and} \quad A^k s_2^i = e^{\lambda_1^k t} s_2^i.$$

So, the condition on the **C2** holds iff the eigenvalues of the common eigenvectors are the same. This establishes that well-posedness is equivalent to either one of **C1** and **C2**. □

Eventually, for the simple repeated eigenvalue, trajectories will remain inside the mode and move along the eigenvector for all the initial states starts inside and on the border of the mode. Hence, the sign of this type of mode is always zero and may be well-posed when it is neighbored by the real distinct and repeated case when condition for singular observability matrix holds.

Remark 3.2.1 *It was already known (see [18]) that, if sliding modes are not allowed, then the elegant condition of Imura and van der Schaft [26] for well-posedness of bimodal systems in terms of modal observability matrices applies also to two adjacent planar modes of our conewise system without any change. We have shown Theorem 3.2.1 that this fact also applies even when sliding modes are allowed.*

3.3 Graph Representation

We now list the graph representations for every mode of a distinct character, i.e., sink, source, half-sink, and transitive including sliding modes. Then, we see how to create the corresponding graph of a given system (2.1) using the component graphs.

Definition 3.3.1 *A node is a cone into or out of which trajectories flow. It is thus natural to designate i) the interior of each sector that has boundaries consisting of a border and/or an eigenvector as a node, designated as an m-node and ii) a ray along an eigenvector as a node, designated as a* $0/\infty$*-node.*

Consider a sink mode that is represented by (Fig.3.1) in case it has no eigenvector on any of its borders. Recall that a mode is a sink iff the larger eigenvector $\mathbf{v}_1$ is inside the cone and the smaller $\mathbf{v}_2$ is external to the cone. Every trajectory that starts in either one of the two sectors $cone\{\mathbf{v}_1, \mathbf{s}_1\}$ and $cone\{\mathbf{v}_1, \mathbf{s}_2\}$ will end up along $\mathbf{v}_1$ so that the two sectors are represented by two nodes $\mathbf{m}_{11}$ and $\mathbf{m}_{12}$. Those that start on the ray $cone\{\mathbf{v}_1\}$ will remain on the same ray either converging to the origin or diverging to infinity so that $cone\{\mathbf{v}_1\}$ is represented by a node denoted by $0/\infty$. The limiting case for a sink is the case when $\mathbf{v}_1$ is at one border and $\mathbf{v}_2$ is external to the cone. In this cae, the two sectors of the previous case collapses to one node yielding the representation (Fig.3.2).

A source mode, on the other hand has the representation (Fig.3.3), which again has two nodes $\mathbf{m}_{11}$ and $\mathbf{m}_{12}$ corresponding to the two sectors $cone\{\mathbf{v}_2, \mathbf{s}_1\}$ and $cone\{\mathbf{v}_2, \mathbf{s}_2\}$. There is also a third node in a source since $cone\{\mathbf{v}_1\}$ is represented by a $0/\infty$ node. The number of nodes are also reduced to two in the limiting case of a source when the eigenvector $\mathbf{v}_2$ is at a boundary (Fig.3.4).

A half sink has both eigenvectors interior to its cone so that there are three sectors represented by the nodes $\mathbf{m}_{11}$-$\mathbf{m}_{13}$ in addition to two $0/\infty$ nodes that represent the two rays along the two eigenvectors. We have thus five nodes in total for the half-sink case as illustrated by (Fig.3.5). The number of nodes are reduced to four in the limiting cases when one of the eigenvectors is on one border.

We only need a simple node for the transitive mode that shows that the trajectories will enter the mode from one side and exit from the other (Fig.3.5).

Finally, for simple-repeated eigenvalues, we only have the $0/\infty$ mode because any trajectory starting from any point will go to zero or infinity along with the initial vector (Fig.3.6), in which the two eigenvectors, that can actually be any two linearly independent vectors, are shown to be inside the cone.

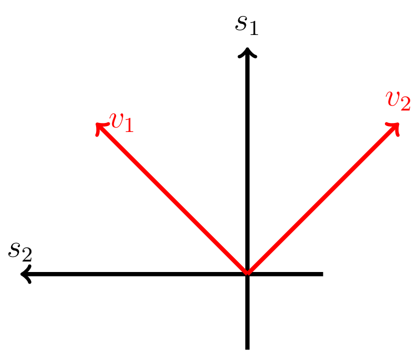

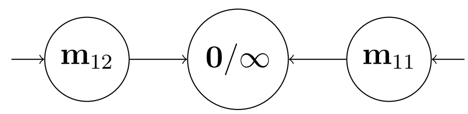

Figure 3.1: Graph representation of a **sink**

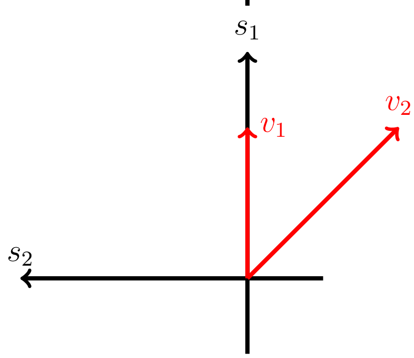

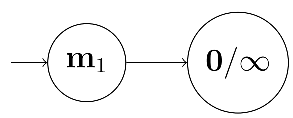

Figure 3.2: Graph representation of **sink** with an eigenvector on the border

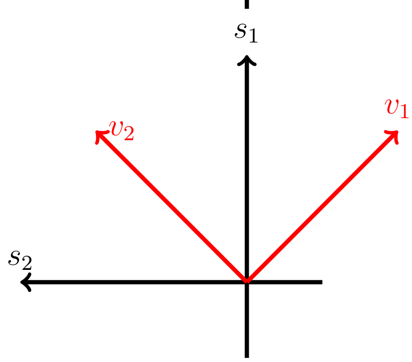

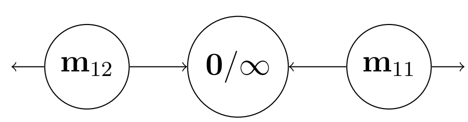

Figure 3.3: Graph representation of a **source**

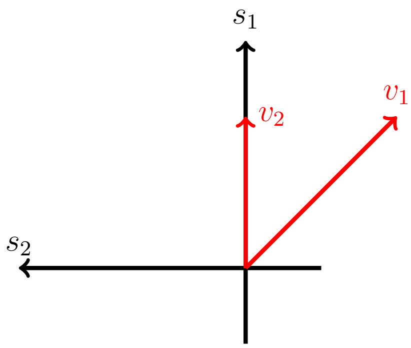

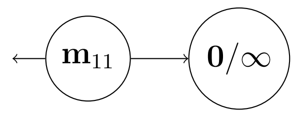

Figure 3.4: Graph representation of **source** with an eigenvector on the border

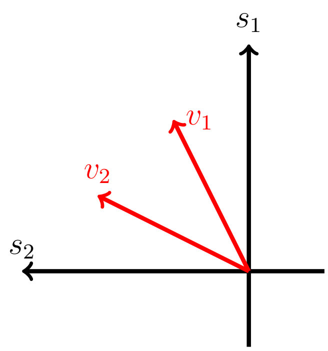

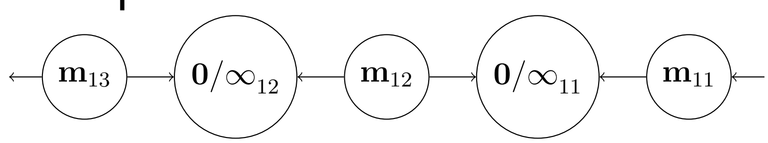

Figure 3.5: Graph representation of a **half-sink**

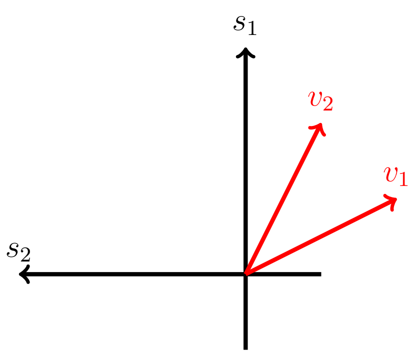

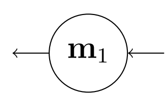

Figure 3.6: Graph representation of **transitive**

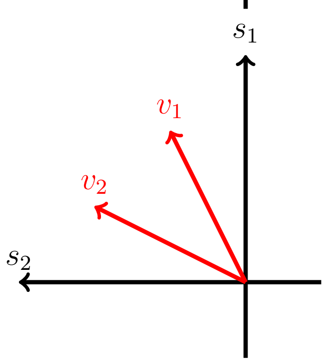

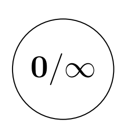

Figure 3.7: Graph representation for the **simple repeated** case

3.4 Reduction Process

In obtaining the corresponding graph of a multi-mode system 2.1, we will encounter a situation where there are two or more adjacent $0/\infty$ nodes. This can occur, for instance, when two neighbor modes both have one eigenvector at the common border or in the case when one node has an eigenvector at its common border with a mode of simple-repeated eigenvalues. In such cases, the trajectories that end up at that border will stay there and travel to infinity or zero. This means that we can depict those two adjacent $0/\infty$ nodes with just one node. A reduction procedure need then be applied.

Remark 3.4.1 *Before beginning the reduction process, we must guarantee that the two* $0/\infty$ *nodes in the neighborhood have the same eigenvalues.*

The reduced form is simply obtained as shown in the figure (3.8), where the two adjacent $0/\infty$ nodes (with incoming edges only) are replaced by one node while the rest of the graph remains unchanged.

Example 3.4.1 *The graph below depicts a system with four modes and two adjacent* $0/\infty$ *modes. The graph before reduction, figure(3.8)(a), gived the graph in part (b) after reduction.*

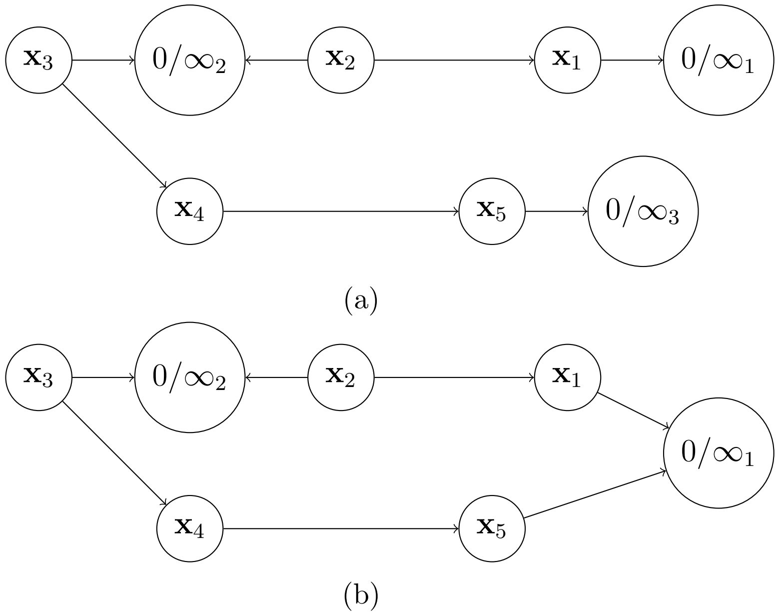

Figure 3.8: Graph representations four mode system(a) reduced version(b).

Remark 3.4.2 *If there are more than two adjacent* $0/\infty$ *nodes, then the reduction procedure need be applied iteratively pair by pair until all adjacent nodes are reduced to one node.*

This graphical reduction process can be described as a matrix reduction process on the adjacency matrix. Note that, because there are no outgoing trajectories from the $0/\infty$ nodes, the associated row of such a node is a zero row. The process consists of the following column operations on the adjacency matrix:

1. Add the higher indexed column of a $0/\infty$ node to the lower indexed $0/\infty$ column and
2. delete the higher indexed $0/\infty$ column and the same indexed row of the adjacency matrix.

The procedure results in an adjacency matrix (of one less size) of the reduced graph.

As an example, suppose two columns and rows of indices i and j (i¡j) in the adjacency matrix belong to two $0/\infty$ nodes. In that case, we will add column j to column i, then delete column and row of index j.

Example 3.4.2 *From the example 3.4.1 we have the following adjacency matrix*

$$A_{adj} = \begin{array}{c} \\ 0/\infty_1 \\ x_1 \\ x_2 \\ 0/\infty_2 \\ x_3 \\ x_4 \\ x_5 \\ 0/\infty_3 \end{array} \begin{array}{c} \begin{array}{cccccccc} 0/\infty_1 & x_1 & x_2 & 0/\infty_2 & x_3 & x_4 & x_5 & 0/\infty_3 \end{array} \\ \begin{pmatrix} 0 & 0 & 0 & 0 & 0 & 0 & 0 & 0 \\ 1 & 0 & 0 & 0 & 0 & 0 & 0 & 0 \\ 0 & 1 & 0 & 1 & 0 & 0 & 0 & 0 \\ 0 & 0 & 0 & 0 & 0 & 0 & 0 & 0 \\ 0 & 0 & 0 & 1 & 0 & 1 & 0 & 0 \\ 0 & 0 & 0 & 0 & 0 & 0 & 1 & 0 \\ 0 & 0 & 0 & 0 & 0 & 0 & 0 & 1 \\ 0 & 0 & 0 & 0 & 0 & 0 & 0 & 0 \end{pmatrix} \end{array}$$

The first and the last nodes are the adjacent $0/\infty$ nodes. We first add the last column to the first and delete the last column and the last row. The reduced matrix is then.

$$A_{adjreduced} = \begin{array}{c} \\ 0/\infty_1 \\ x_1 \\ x_2 \\ 0/\infty_2 \\ x_3 \\ x_4 \\ x_5 \end{array} \begin{array}{c} \begin{array}{ccccccc} 0/\infty_1 & x_1 & x_2 & 0/\infty_2 & x_3 & x_4 & x_5 \end{array} \\ \begin{pmatrix} 0 & 0 & 0 & 0 & 0 & 0 & 0 \\ 1 & 0 & 0 & 0 & 0 & 0 & 0 \\ 0 & 1 & 0 & 1 & 0 & 0 & 0 \\ 0 & 0 & 0 & 0 & 0 & 0 & 0 \\ 0 & 0 & 0 & 1 & 0 & 1 & 0 \\ 1 & 0 & 0 & 0 & 0 & 0 & 1 \\ 0 & 0 & 0 & 0 & 0 & 0 & 0 \end{pmatrix} \end{array}$$

Note that the adjacent nodes do not always have to be the initial and final nodes as any symmetric permutation of rows and columns of the adjacency matrix will correspond to a renumbering of nodes.

We can now state our graphical necessary and sufficient condition on well-posedness of (2.1).

Theorem 3.4.1 *System (2.1) is well-posed if and only if one of the equivalent conditions **I** and **II** holds:*

***I**. The corresponding reduced directed graph is 2-regular (degree of each node is two) and is weakly-connected.*

***II**. The corresponding reduced adjacency matrix A of size n satisfies*

(a)

$$(\sum_{i=1}^{n} a_{ki} + a_{ik}) - a_{kk} = 2,\ k = 1, 2, ...n,$$

(b) there is no symmetric permutation P of columns and rows that gives

$$PAP = \begin{bmatrix} X_1 & . & 0 \\ .. & . & .. \\ 0 & . & X_2 \end{bmatrix}$$

for some square matrices X_1, X_2 of sizes greater than one.

Proof. We first show that the condition **I** is necessary and sufficient for well-posedness. If the reduced graph is not weakly connected, then there are two nodes with no path in between. The graph representations for single modes are all weakly-connected themselves so that, if the reduced graph is not weakly connected, then this corresponds to the case of two modes with no border in between. But this would then give a system (2.1) that is not well-defined because the cones must fill out the plane. Suppose now that, the reduced graph is not 2-regular, then there may be either a node with only one edge, which is not possible since each planar mode has two neighbors and every sector is represented by a node with exactly two edges (following the reduction process, the simple repeated, and the case with an eigenvector on the border will be reduced to a node with two edges), or there is a node with more than two edges. In this latter case we must have at least two incoming or at least two outgoing edges. But, this corresponds to the case of a border either a sliding mode or an initial condition resulting in two distinct trajectories. By our reduction procedure. a sliding mode is represented again by a node with two edges. It follows that, if the graph is not two-regular, then smooth continuation is not possible from at least one border. Fig 3.9 illustrates a graph that corresponds to a case where smooth continuation is not possible from a border.

Conversely, suppose that the system (2.1) is not well-posed so that there is an initial state $\mathbf{b} \in \mathbb{R}^{\mathbf{2}}$, for which smooth continuation is not possible or it is possible for two modes giving solutions that are different for all $t \geq 0$. We can focus our attention at only the initial states at a border $\mathbf{b} \in \mathsf{B}^{\mathbf{k}}_{\mathbf{1}} = \mathsf{B}^{\mathbf{i}}_{\mathbf{2}} =$ between modes i and k. Typical examples of no solution in neither mode i nor k is when both modes are sinks (or half-sinks with both sink sectors containing the border) with no sliding mode. This gives to a graph in which no edge exists between two nodes, i.e., two nodes with degree one or less. The graph is then not two regular. If there are two different solutions that continue in both modes i and k, this corresponds to a typical case of two sources (or half-sinks with transitive sectors of different directions containing the border). This gives a graph with two nodes of degree three since two neighboring nodes must outgoing edges connecting to the other, as illustrated in Fig 3.9.b.

(a) (b)

Figure 3.9: Graph representations of multiple solution (a) and no solution (b).

The equivalence of conditions **I** and **II** follows directly by the definition of the adjacency matrix and by our reduction procedure. □

3.4.1 Examples

The following examples applies the Theorem 3.4.1 and determines well-posedness of the system by checking the corresponding directed graph.

Example 3.4.3 *Consider a Conewise linear system with*

$$C^1 = -C^3 = \begin{bmatrix} 1 & 0 \\ 0 & 1 \end{bmatrix}, \quad C^2 = -C^4 = \begin{bmatrix} -1 & 0 \\ 0 & 1 \end{bmatrix}.$$

The state matrices for the CLS are given as

$$A^1 = A^2 = \begin{bmatrix} -2.5 & -0.5 \\ -0.5 & -2.5 \end{bmatrix}, \quad A^3 = \begin{bmatrix} \frac{7}{3} & \frac{2}{3} \\ -\frac{2}{3} & \frac{2}{3} \end{bmatrix}, \quad A^4 = \begin{bmatrix} \frac{2}{3} & \frac{2}{3} \\ -\frac{2}{3} & \frac{7}{3} \end{bmatrix}.$$

The eigenvectors for each mode can be chosen as

$$V^1 = V^2 = \begin{bmatrix} -1 & 1 \\ 1 & 1 \end{bmatrix}, \quad V^3 = \begin{bmatrix} -1 & -0.5 \\ 0.5 & 1 \end{bmatrix}, \quad V^4 = \begin{bmatrix} 0.5 & 1 \\ 1 & 0.5 \end{bmatrix}.$$

As we can see in the Figure 3.18 if we start from different initial points in any modes there exists a unique solution and smooth continuation is possible from every initial mode. In Figure 3.11 directed graph corresponding to this system is shown which is weakly connected and 2-regular as well.

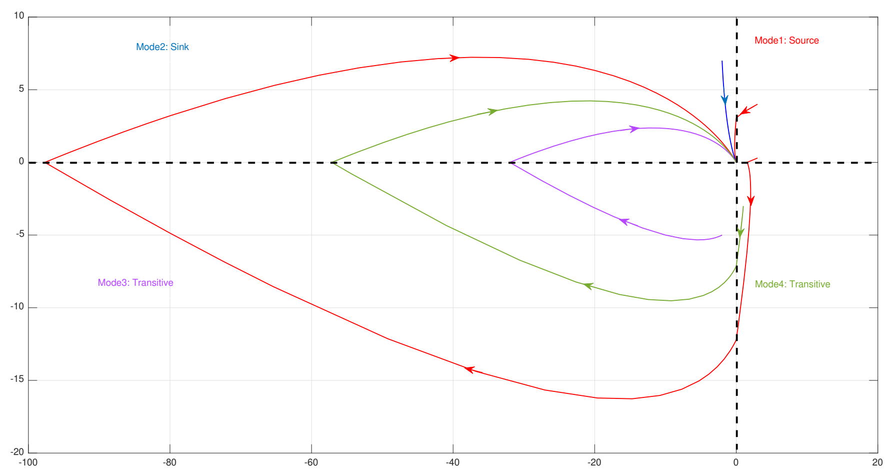

Figure 3.10: Trajectory movements in the system of Example 3.4.3

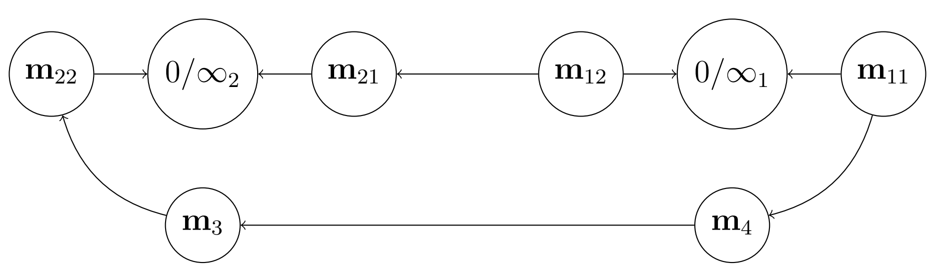

Figure 3.11: Graph representations of well-posed system.

$$
A_{adjreduced} = \begin{array}{c} \\ m_{11} \\ 0/\infty_1 \\ m_{12} \\ m_{21} \\ 0/\infty_2 \\ m_{22} \\ m_3 \\ m_4 \end{array}
\begin{array}{c}
\begin{array}{cccccccc} m_{11} & 0/\infty_1 & m_{12} & m_{21} & 0/\infty_2 & m_{22} & m_3 & m_4 \end{array} \\
\begin{pmatrix}
0 & 1 & 0 & 0 & 0 & 0 & 0 & 1 \\
0 & 0 & 0 & 0 & 0 & 0 & 0 & 0 \\
0 & 1 & 0 & 1 & 0 & 0 & 0 & 0 \\
0 & 0 & 0 & 0 & 1 & 0 & 0 & 0 \\
0 & 0 & 0 & 0 & 0 & 0 & 0 & 0 \\
0 & 0 & 0 & 0 & 1 & 0 & 0 & 0 \\
0 & 0 & 0 & 0 & 0 & 1 & 0 & 0 \\
0 & 0 & 0 & 0 & 0 & 0 & 1 & 0
\end{pmatrix}
\end{array}
$$

Example 3.4.4 *Consider a Conewise linear system with*

$$
C^1 = -C^3 = \begin{bmatrix} 1 & 0 \\ 0 & 1 \end{bmatrix}, \quad C^2 = -C^4 = \begin{bmatrix} -1 & 0 \\ 0 & 1 \end{bmatrix}.
$$

The state matrices for the CLS are given as

$$
A^1 = A^2 = A^3 = \begin{bmatrix} -2.5 & -0.5 \\ -0.5 & -2.5 \end{bmatrix}, \quad A^4 = \begin{bmatrix} \frac{7}{3} & -\frac{2}{3} \\ \frac{2}{3} & \frac{2}{3} \end{bmatrix}.
$$

The eigenvectors for each mode can be chosen as

$$
V^1 = V^2 = V^3 = \begin{bmatrix} -1 & 1 \\ 1 & 1 \end{bmatrix}, \quad V^4 = \begin{bmatrix} 1 & 0.5 \\ 0.5 & 1 \end{bmatrix}.
$$

In this example as we can see from Figure 3.12 the smooth continuation is not possible from the first and fourth mode the trajectories which starts in the fourth mode will reach to the common border with first mode and same happens to the trajectories which start in the first mode. On the other hand, if we starts on the common border the trajectory will not stay on the border, therefore, the smooth continuation is not possible and the system is not well-posed. This situation will lead to have the corresponding graph 3.13 and it is not 2-regular anymore. Also the corresponding adjacency matrix has the sum of 3 for the m_{11} *and* m_4 *row and column.*

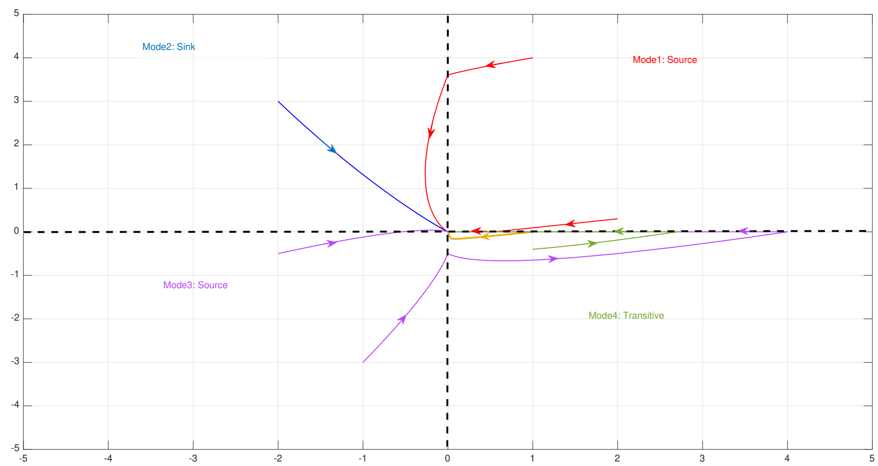

Figure 3.12: Trajectories movement in a not well-posed system

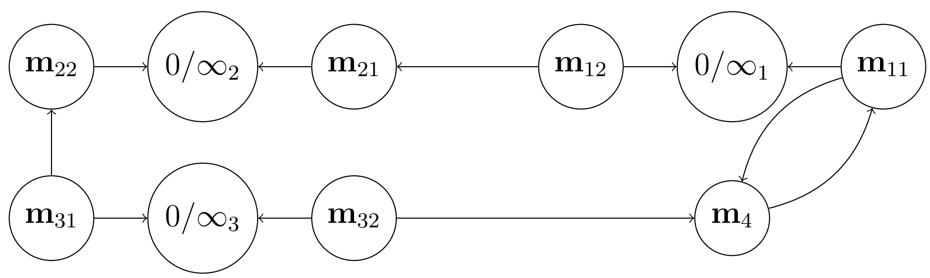

Figure 3.13: Graph representations of a not well-posed system.

$$A_{adjreduced} = \begin{array}{r} \\ m_{11} \\ 0/\infty_1 \\ m_{12} \\ m_{21} \\ 0/\infty_2 \\ m_{22} \\ m_{31} \\ 0/\infty_3 \\ m_{32} \\ m_4 \end{array} \begin{array}{c} \begin{array}{cccccccccc} m_{11} & 0/\infty_1 & m_{12} & m_{21} & 0/\infty_2 & m_{22} & m_{31} & 0/\infty_3 & m_{32} & m_4 \end{array} \\ \begin{pmatrix} 0 & 1 & 0 & 0 & 0 & 0 & 0 & 0 & 0 & 1 \\ 0 & 0 & 0 & 0 & 0 & 0 & 0 & 0 & 0 & 0 \\ 0 & 1 & 0 & 1 & 0 & 0 & 0 & 0 & 0 & 0 \\ 0 & 0 & 0 & 0 & 1 & 0 & 0 & 0 & 0 & 0 \\ 0 & 0 & 0 & 0 & 0 & 0 & 0 & 0 & 0 & 0 \\ 0 & 0 & 0 & 0 & 1 & 0 & 0 & 0 & 0 & 0 \\ 0 & 0 & 0 & 0 & 0 & 1 & 0 & 1 & 0 & 0 \\ 0 & 0 & 0 & 0 & 0 & 0 & 0 & 0 & 0 & 0 \\ 0 & 0 & 0 & 0 & 0 & 0 & 0 & 1 & 0 & 1 \\ 1 & 0 & 0 & 0 & 0 & 0 & 0 & 0 & 0 & 0 \end{pmatrix} \end{array}$$

The next example illustrates the reduction procedure that need to be applied when two adjacent $0/\infty$ nodes occur in a graph.

Example 3.4.5 *Consider a CLS with*

$$C^1 = -C^3 = \begin{bmatrix} 1 & 0 \\ 0 & 1 \end{bmatrix}, \quad C^2 = -C^4 = \begin{bmatrix} -1 & 0 \\ 0 & 1 \end{bmatrix}.$$

The state matrices for the CLS are given as

$$A^1 = \begin{bmatrix} -1 & \frac{-1}{2} \\ 0 & -2 \end{bmatrix}, \quad A^2 = \begin{bmatrix} \frac{-5}{3} & \frac{-1}{3} \\ \frac{-2}{3} & \frac{-4}{3} \end{bmatrix}, \quad A^3 = \begin{bmatrix} \frac{-5}{3} & \frac{10}{3} \\ \frac{-10}{3} & \frac{11}{3} \end{bmatrix}, \quad A^4 = \begin{bmatrix} -2 & \frac{1}{2} \\ 0 & -1 \end{bmatrix},$$

The eigenvectors for each mode can be chosen as

$$V^1 = \begin{bmatrix} 1 & 1 \\ 0 & 2 \end{bmatrix}, \quad V^2 = \begin{bmatrix} -1 & 1 \\ 2 & 1 \end{bmatrix}, \quad V^3 = \begin{bmatrix} 2 & 1 \\ 1 & 2 \end{bmatrix}, \quad V^4 = \begin{bmatrix} -1 & 2 \\ -2 & 0 \end{bmatrix},$$

In this example, we have four modes: sink, source, transitive (non-real), and half-sink. As we can see from the Λ matrix for each mode.

$$\Lambda^1 = \begin{bmatrix} -1 & 0 \\ 0 & -2 \end{bmatrix}, \Lambda^2 = \begin{bmatrix} -1 & 0 \\ 0 & -2 \end{bmatrix}, \Lambda^3 = \begin{bmatrix} 1 & 2 \\ -2 & 1 \end{bmatrix}, \Lambda^4 = \begin{bmatrix} -1 & 0 \\ 0 & -2 \end{bmatrix},$$

According to the Figure 3.14, every trajectory that begins at the common boundary of Mode-4 and Mode-1 will remain on the border. The trajectories that start in the interior of the modes will finish up in the sink mode. The Figure 3.16, on the other hand, shows the reduced form of the graph representing the system, which is 2-regular and weakly-connected.

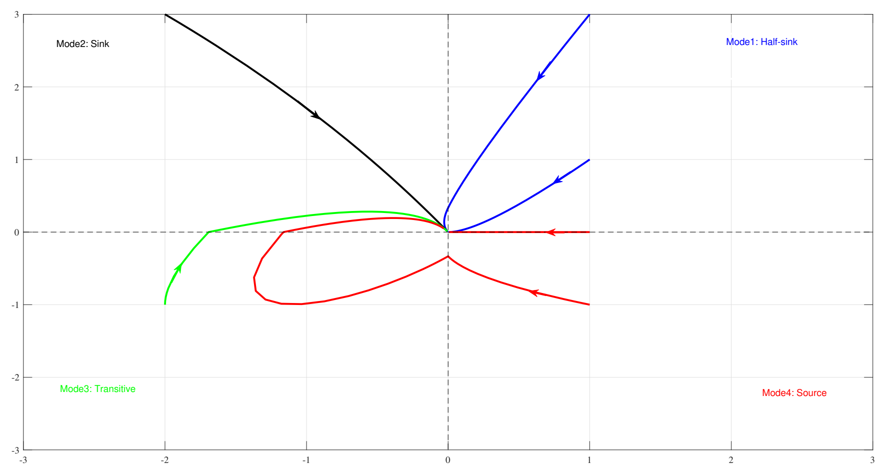

Figure 3.14: Trajectories movement for a well-posed system with seven modes

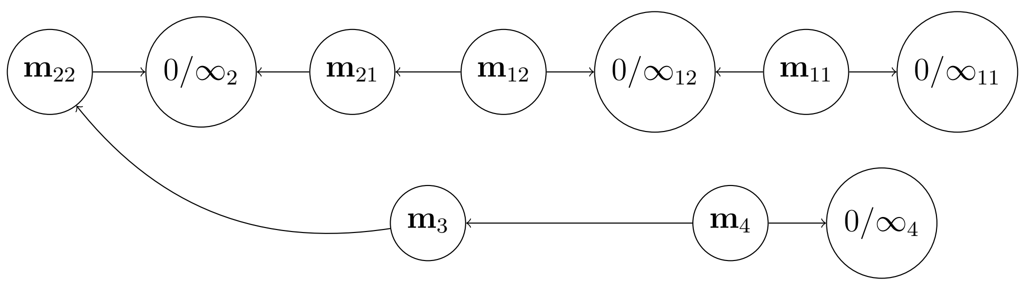

Figure 3.15: Graph representations of the system with two $0/\infty$ modes

$$A_{adjreduced} = \begin{array}{c} \\ 0/\infty_{11} \\ m_{11} \\ 0/\infty_{12} \\ m_{12} \\ m_{21} \\ 0/\infty_{2} \\ m_{22} \\ m_3 \\ m_4 \end{array} \begin{array}{c} \begin{array}{ccccccccc} 0/\infty_{11} & m_{11} & 0/\infty_{12} & m_{12} & m_{21} & 0/\infty_{2} & m_{22} & m_3 & m_4 \end{array} \\ \begin{pmatrix} 0 & 0 & 0 & 0 & 0 & 0 & 0 & 0 & 0 \\ 1 & 0 & 1 & 0 & 0 & 0 & 0 & 0 & 0 \\ 0 & 0 & 0 & 0 & 0 & 0 & 0 & 0 & 0 \\ 0 & 0 & 1 & 0 & 1 & 0 & 0 & 0 & 0 \\ 0 & 0 & 0 & 0 & 0 & 1 & 0 & 0 & 0 \\ 0 & 0 & 0 & 0 & 0 & 0 & 0 & 0 & 0 \\ 0 & 0 & 0 & 0 & 0 & 1 & 0 & 0 & 0 \\ 0 & 0 & 0 & 0 & 0 & 0 & 1 & 0 & 0 \\ 1 & 0 & 0 & 0 & 0 & 0 & 0 & 1 & 0 \end{pmatrix} \end{array}$$

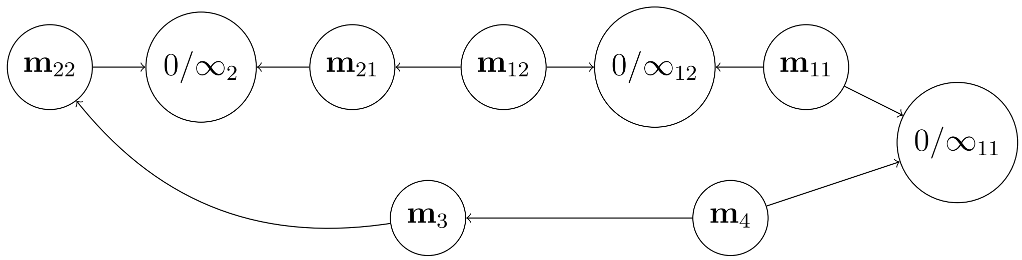

Figure 3.16: Reduced graph representations of the system with two $0/\infty$ modes in close proximity

3.5 Stability

The system (2.1) is Globally Asymptotically Stable (or simply, stable) if all trajectories decay to the origin as $t \to \infty$, i.e., if for all $\mathbf{b} \in \mathbf{R^2}, \lim_{\mathbf{t}\to\infty} \mathbf{x}(\mathbf{t}, \mathbf{b}) = \mathbf{0}$.

Lyapunov-based technique is widely used in studying the stability of piecewise linear systems, but the requirement to devise a common Lyapunov function for all modes quickly brings this method to a halt. A complete necessary and sufficient condition for stability of (2.1) exists and is first obtained by [6]. In [18], an equivalent version of the condition was obtained.

In what follows, we first review the definition of *factor of expansion*, which is a measure of the distance of the trajectory to the origin at a border B_1^i or B_2^i of a transitive cone. It is the natural logarithm of the gain $\frac{|x|}{|s^k|}$ a trajectory goes through when it begins at a border B^i and travels through the entire sector, eventually reaching the other border B^k.

Definition 3.5.1 *If a mode i is transitive, then its factor of expansion (FEX) is*

$$F^i := \begin{cases} ln\frac{|{}^i v\times s_1^i|}{|{}^i v\times s_2^i|} + \mu^i t_2^i & \textit{if it is positive-transitive,} \\ ln\frac{|{}^i v\times s_2^i|}{|{}^i v\times s_1^i|} + \mu^i t_1^i & \textit{if it is negative-transitive,} \end{cases} \tag{3.4}$$

where μ^i is λ_1^i or σ^i, ^{i}v denote v_1^i or $v_1^i + jv_2^i$ in case of real or non-real eigenvalues, respectively. Also $t_1^i(t_2^i)$ is called *regime time* which is the time it takes the trajectory to move from s_2^i to s_1^i(s_1^i to s_2^i).

$$t_1^i = \begin{cases} \frac{1}{\lambda_1^i - \lambda_2^i} ln \frac{\left|n_{22}^i(s_2^i)\right|}{\left|n_{21}^i(s_2^i)\right|} & \text{for real and distinct eigenvalues ,} \\ \frac{\left|n_{21}^i(s_2^i)+n_{22}^i(s_2^i)\right|}{\left|((c_2^i)^T v_1^i)((w_2^i)^T s_2^i)\right|} & \text{for real and repeated eigenvalues,} \\ \frac{\Theta^i}{\omega^i} & \text{for non-real eigenvalues} \end{cases} \tag{3.5}$$

where,

$$\Theta^i := \tan^{-1} \frac{(c_2^i)^T s_2^i}{(c_2^i)^T v_2^i (w_1^i)^T s_2^i - (c_2^i)^T v_1^i (w_2^i)^T s_2^i}. \tag{3.6}$$

Consequently,

$$t_2^i = \begin{cases} \frac{1}{\lambda_1^i - \lambda_2^i} ln \frac{\left|n_{12}^i(s_1^i)\right|}{\left|n_{11}^i(s_1^i)\right|} & \text{for real and distinct eigenvalues ,} \\ \frac{\left|n_{11}^i(s_1^i)+n_{12}^i(s_1^i)\right|}{\left|((c_1^i)^T v_1^i)((w_2^i)^T s_1^i)\right|} & \text{for real and repeated eigenvalues,} \\ \frac{\Theta^i}{\omega^i} & \text{for non-real eigenvalues} \end{cases} \tag{3.7}$$

where,

$$\Theta^i := \tan^{-1} \frac{(c_2^i)^T s_1^i}{(c_2^i)^T v_2^i (w_1^i)^T s_1^i - (c_2^i)^T v_1^i (w_2^i)^T s_1^i}. \tag{3.8}$$

With the help of our well-posedness result, we can now rewrite theorem 5.2.1 from [18].

Theorem 3.5.1 *A well-posed conewise linear system 2.1 is globally asymptotically stable if and only if when the reduced graph is acyclic, the eigenvalues corresponding to* $0/\infty$ *nodes are all negative and when the reduced graph is cyclic,* $F = \sum_{i=1}^{m} F^i < 0$*, where* m *is the number of modes.*

Proof. If a 2-regular, connected, and directed graph has a cycle, then it must be a cycle graph, i.e., the cycle should include all its nodes. It follows that the conditions of the theorem covers all cases. If the graph is acyclic, then all paths terminate at a $0/\infty$ node, where the trajectories move radially along an eigenvector. The corresponding eigenvalue must then be negative, in order for the trajectory to converge to zero. If the graph is a cycle, so that it contains no $0/\infty$ node and all nodes correspond to modes that are transitive in the same direction. Then, for a trajectory to converge to zero, it is necessary and sufficient that starting at one border with an initial vector $\mathbf{b}$, completing one cycle, and hitting the border of start, the trajectory ends closer to the origin than $\mathbf{b}$. The sum of the expansion factors gives the logarithm of the ratio of the length of final value of the trajectory after one cycle to $\mathbf{b}$. Hence, the trajectory asymptotically converges to zero if and only if $F = \sum_{i=1}^{m} F^i < 0$. $\square$

Example 3.5.1 *Consider a CLS with*

$$C^1 = -C^3 = \begin{bmatrix} 1 & 0 \\ 0 & 1 \end{bmatrix}, \quad C^2 = -C^4 = \begin{bmatrix} 0 & 1 \\ -1 & 0 \end{bmatrix}.$$

The state matrices for the CLS are given as

$$A^1 = \begin{bmatrix} \frac{-7}{3} & \frac{-2}{3} \\ \frac{2}{3} & \frac{-2}{3} \end{bmatrix}, \quad A^2 = \begin{bmatrix} \frac{11}{3} & \frac{-10}{3} \\ \frac{10}{3} & \frac{-5}{3} \end{bmatrix}, \quad A^3 = \begin{bmatrix} \frac{-5}{3} & \frac{-4}{3} \\ \frac{1}{3} & \frac{-1}{3} \end{bmatrix}, \quad A^4 = \begin{bmatrix} \frac{-2}{3} & \frac{-2}{3} \\ \frac{2}{3} & \frac{-7}{3} \end{bmatrix}.$$

The eigenvectors for each mode can be chosen as

$$V^1 = \begin{bmatrix} -1 & -2 \\ 2 & 1 \end{bmatrix}, \quad V^2 = \begin{bmatrix} 1 & 2 \\ 2 & 1 \end{bmatrix}, \quad V^3 = \begin{bmatrix} -2 & -1 \\ 1 & -2 \end{bmatrix}, \quad V^4 = \begin{bmatrix} -2 & -1 \\ -1 & -2 \end{bmatrix},$$

and it can be checked that we have four positively oriented modes. The Lambda matrices are

$$\Lambda^1 = \begin{bmatrix} -1 & 0 \\ 0 & -2 \end{bmatrix}, \Lambda^2 = \begin{bmatrix} 1 & 2 \\ -2 & 1 \end{bmatrix}, \Lambda^3 = \begin{bmatrix} -1 & 1 \\ 0 & -1 \end{bmatrix}, \Lambda^4 = \begin{bmatrix} -1 & 0 \\ 0 & -2 \end{bmatrix},$$

so that they are a mixture of three types of Jordan forms.

$$\begin{tikzcd} \mathbf{m}_2 \arrow[d] & \mathbf{m}_1 \arrow[l] \\ \mathbf{m}_3 \arrow[r] & \mathbf{m}_4 \arrow[u] \end{tikzcd}$$

Figure 3.17: Graph representations of the cyclic system of Example 3.5.1

According to Theorem 3.2.1 and Figure 3.17 the system is well-posed. This can also be checked through the adjacency matrix below, which also gives that the *system is cyclic; as $A^4 = \mathbb{I}^4$ is the identity matrix so that it is not nilpotent.*

$$A_{adj} = \begin{array}{c} \\ m_1 \\ m_2 \\ m_3 \\ m_4 \end{array} \begin{array}{c} \begin{array}{cccc} m_1 & m_2 & m_3 & m_4 \end{array} \\ \begin{pmatrix} 0 & 1 & 0 & 0 \\ 0 & 0 & 1 & 0 \\ 0 & 0 & 0 & 1 \\ 1 & 0 & 0 & 0 \end{pmatrix} \end{array}$$

The system is stable if and only if the $F < 0$ according to the Theorem 3.5.1. Because all of the modes in our example are positively orientated, we utilize the $F = \sum_{i=1}^{m} F^i < 0$ to check the F for each one. F1=-0.69314, F2=0, F3=-1.09861, and F4=-0.69314, resulting in F=-2.48489, a negative value, thus the system is globally asymptotically stable.

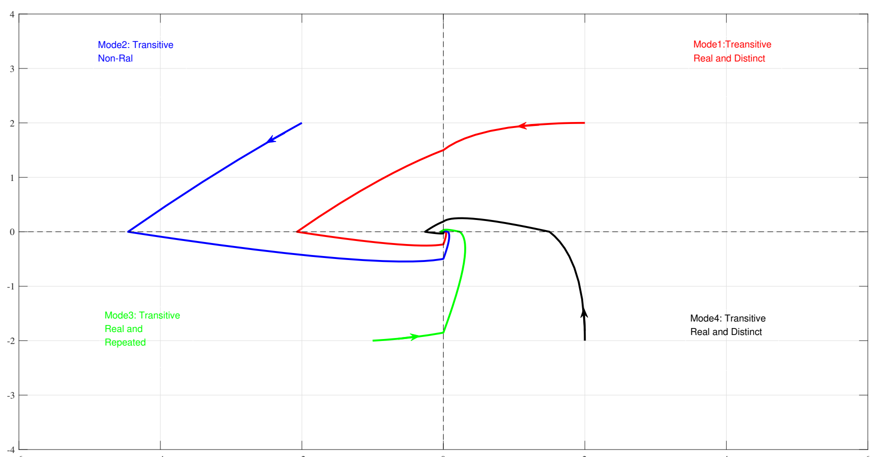

Figure 3.18: Sample trajectory movements for the system of Example 3.5.1

Chapter 4

Conclusions and Future Work

We have examined well-posedness of a multi-modal conewise linear system in which each mode is defined on a polyhedral cone and can have its dynamic defined by an A-matrix having any one of the possible Jordan forms. We have also allowed sliding modes by also considering modes with observability matrices that can be singular.

We have adopted Caratheodory based solution concept for the conewise system and used the smooth continuation version of the well-posedness definition. It was already known that, if sliding modes are not allowed, then the elegant condition of well-posedness for bimodal systems in terms of modal observability matrices applies also to two adjacent planar modes of our conewise system without any change. We have shown in this thesis that this fact also applies even when sliding modes are allowed.

A graphical condition has also been given for the well-posedness of the overall conewise system with an arbitrary number of modes. This approach, strictly speaking, is not necessary since planar systems have a very simple interconnection structure. Nevertheless, we have shown that the graph of even our planar system helps to consider well-posedness and stability issues in a unified manner. We have thus stated the well-known condition for stability with the help of the graph representation and a special reduction procedure applies to the initial graph. This graphical result may be helpful in well-posedness studies of conewise systems of higher dimensions.

Our immediate future work will be an extension of these results to spatial (3D) conewise systems.

Bibliography

[1] P. J. Antsaklis, "Special issue on hybrid systems: Theory and applications a brief introduction to the theory and applications of hybrid systems,," *IEEE*, vol. 88, no. 7, pp. 879–887, 2000.

[2] R. L. Grossman, A. Nerode, A. P. Ravn, and H. Rischel, "Hybrid systems," *Berlin, Germany: Springer-Verlag*, vol. 736, 1993.

[3] L. Rodrigues and J. P. How, "Observer-based control of piecewise-affine systems," *International Journal of Control*, vol. 76, no. 5, pp. 459–477, 2003.

[4] J. Xu and L. Xie, *Control and estimation of piecewise affine systems.* Elsevier, 2014.

[5] D. M. W. LeenaertsWim and M. G. V. Bokhoven, *Piecewise Linear Modeling and Analysis.* K1uwer Academic Publishers, 1998.

[6] Y. Iwatani and S. Hara, "Stability tests and stabilization for piecewise linear systems based on poles and zeros of subsystems," *Automatica*, vol. 42, no. 10, pp. 1685–1695, 2006.

[7] M. Camlibel, J. Pang, and J. Shen, "Conewise linear systems: Non-zenoness and observability," *SIAM Journal on Control and Optimization*, vol. 45, no. 5, pp. 1769–1800, 2006.

[8] Z. Sun, "Stability and contractivity of conewise linear systems," *2010 IEEE International Symposium on Intelligent Control*, pp. 2094–2098, 2010.

[9] A. B. Özgüler and M. Zakwan, "Conewise linear systems: A characterization of transitive cones in 3d-space," *2019 18th European Control Conference (ECC)*, pp. 3692–3697, 2019.

[10] I. Raffaele, V. Francesco, and I. Luigi, "Stability analysis of conewise linear systems with sliding modes," *2015 54th IEEE Conference on Decision and Control (CDC)*, pp. 1174–1179, 2015.

[11] A. Arapostathis and M. E. Broucke, "Stability and controllability of planar, conewise linear systems," *2007 46th IEEE Conference on Decision and Control*, pp. 6268–6273, 2007.

[12] B. Samadi and L. Rodrigues, "A unified dissipativity approach for stability analysis of piecewise smooth systems," *Automatica*, vol. 47, no. 12, pp. 2735–2742, 2011.

[13] Y. Mori, T. Mori, and Y. Kuroe, "A solution to the common lyapunov function problem for continuous-time systems," *Proceedings of the 36th IEEE Conference on Decision and Control*, vol. 4, pp. 3530–3531, 1997.

[14] M. Wicks, P. Peleties, and R. DeCarlo, "Construction of piecewise lyapunov functions for stabilizing switched systems," *Proceedings of 1994 33rd IEEE Conference on Decision and Control*, vol. 4, pp. 3492–3497, 1994.

[15] M. Johansson and A. Rantzer, "Computation of piecewise quadratic lyapunov functions for hybrid systems," *IEEE Transactions on Automatic Control*, vol. 43, no. 4, pp. 555–559, 1998.

[16] A. Hassibi and S. Boyd, "Quadratic stabilization and control of piecewise-linear systems," *Proceedings of the 1998 American Control Conference. ACC (IEEE Cat. No.98CH36207)*, vol. 6, pp. 3659–3664, 1998.

[17] Z. Sun, "Stability of piecewise linear systems revisited," *Annual Reviews in Control, Elsevier*, vol. 34, no. 2, pp. 221–231, 2010.

[18] A. Abdullahi, "Stability of planar piecewise linear systems: A geometric approach," Master's thesis, Bilkent University, 2015.

[19] A. van der Schaft and H. Schumacher, *An Introduction to Hybrid Dynamical Systems.* Volume 251 of Lecture Notes in Control and Information Sciences, Springer, 2000.

[20] G. Şahan and V. Eldem, "Well posedness conditions for bimodal piecewise affine systems," *Systems & Control Letters*, vol. 83, pp. 9–18, 2015.

[21] M. Çamhbel and J. Schumacher, "Well-posedness of a class of piecewise linear systems," *1999 European Control Conference (ECC)*, pp. 3112–3117, 1999.

[22] W. Heemels, J. Schumacher, and S. Weiland, "Well-posedness of linear complementarity systems," *Proceedings of the 38th IEEE Conference on Decision and Control (Cat. No.99CH36304)*, vol. 3, pp. 3037–3042, 1999.

[23] L. Thuan and M.K.Camlibel, "On the existence, uniqueness and nature of carathéodory and filippov solutions for bimodal piecewise affine dynamical systems," *Systems & Control Letters*, vol. 68, pp. 76–85, 2014.

[24] J. ichi Imura, "Well-posedness analysis of switch-driven piecewise affine systems," *IEEE Transactions on Automatic Control*, vol. 48, no. 11, pp. 1926–1935, 2003.

[25] Y. Lootsma, A. van der Schaft, and M. Camlibel, "Uniqueness of solutions of relay systems," *Automatica*, vol. 35, no. 3, pp. 467–478, 1999.

[26] J.-i. Imura and A. Van Der Schaft, "Characterization of well-posedness of piecewise-linear systems," *IEEE Transactions on Automatic Control*, vol. 45, no. 9, pp. 1600–1619, 2000.

[27] X. Xia, "Well posedness of piecewise-linear systems with multiple modes and multiple criteria," *IEEE Transactions on Automatic Control*, vol. 47, no. 10, pp. 1716–1720, 2002.

[28] G. Şahan and V. Eldem, "Well posedness conditions for planar conewise linear systems," *Transactions of the Institute of Measurement and Control*, vol. 41, no. 8, pp. 2093–2099, 2019.

[29] M. Pachter and D. Jacobson, “The stability of planar dynamical systems linear-in-cones,” *IEEE Transactions on Automatic Control*, vol. 26, no. 2, pp. 587–590, 1981.

[30] G. Şahan, “Existence and uniqueness of solution for discontinuous conewise linear systems,” *IFAC-PapersOnLine*, vol. 53, no. 2, pp. 927–932, 2020.

[31] G. Şahan, “Existence and uniqueness of solution for discontinuous conewise linear systems,” *IFAC-PapersOnLine*, vol. 53, no. 2, pp. 927–932, 2020.

[32] M. Zakwan, “Stability of third order conewise linear systems,” Master’s thesis, Bilkent University, 2019.

[33] G. Chartrand and P. Zhang, *A First Course In Grapgh Theory*. Dover Publications, INC. Mineola, New York, 2012.

[34] A. Dharwadker and S. Pirzada, *Grapgh Theory*. Institute of Mathematics, H-501 P. Vihar, GURGAON, HARYANA 122017, INDIA, 2011.

[35] M. N. S. S. K. Thulasiraman, *Graphs:Theory and Algorithms*. A Wiley-Interscience Publication, 1992.

[36] K. Guo, *Simple eigenvalues of graphs and digraphs*. PhD thesis, University of Waterloo, 2015.

[37] J. ichi Imura, “Well-posedness analysis of switch-driven piecewise affine systems,” *IEEE Transactions on Automatic Control*, vol. 48, no. 11, pp. 1926 – 1935, 2003.

[38] A. van der schaft and J. Schumacher, “The complementary-slackness class of hybrid systems,” *Mathematics of Control, Signals and Systems*, pp. 266–301, 1996.

Appendix A

Matlab Code

```
%This code generates pwl systems for simulation of trajectories
%in various modes. The values are for Example 3.5.1.

clear all
close all
clc
%The Pwl(piecewise linear systems) Toolbox
addpath(genpath('C:\Users\Daniyal\Desktop\apply\pwl'))

% Conewise system 1
Lambda1= [-1 0; 0 -2] ; % eigen values real distinc
x1_1 = [-1 2]' ;
y1_1 = [-2 1]';
V1 = [x1_1  y1_1] ; % eigen-vectors
A1 =  V1*Lambda1*inv(V1); % A matrix for simulation
s1_1= [1 0]';
s1_2 = [0 1]' ;
S1 = [s1_1 s1_2] ;
C1 = inv(S1) ; % C matrix for simulation
W1 = inv(V1) ;

% Conewise system 2
Lambda2= [1 2; -2 1] ; % eigen values real distinc
x2_1 = [1 2]' ;
y2_1 = [2 1]';
```

```
V2 = [x2_1  y2_1] ; % eigen-vectors
A2 =  V2*Lambda2*inv(V2); % A matrix for simulation
s2_1= [0  1]';
s2_2 = [-1  0]' ;
S2 = [s2_1  s2_2] ;
C2 = inv(S2) ; % C matrix for simulation
W2 = inv(V2) ;

% Conewise system 3
Lambda3= [-1  1;  0  -1] ; % eigen values real distinc
x3_1 = [-2  1]' ;
y3_1 = [-1  2]';
V3 = [x3_1  y3_1] ; % eigen-vectors
A3 =  V3*Lambda3*inv(V3); % A matrix for simulation
s3_1= [-1  0]';
s3_2 = [0  -1]' ;
S3 = [s3_1  s3_2] ;
C3 = inv(S3) ; % C matrix for simulation
W3 = inv(V3) ;

% Conewise system 4
Lambda4= [-1  0;  0  -2] ; % eigen values real distinc
x4_1 = [-2  -1]' ;
y4_1 = [-1  -2]';
V4 = [x4_1  y4_1] ; % eigen-vectors
A4 =  V4*Lambda4*inv(V4); % A matrix for simulation
s4_1= [0  -1]';
s4_2 = [1  0]' ;
S4 = [s4_1  s4_2] ;
C4 = inv(S4) ; % C matrix for simulation
W4 = inv(V4) ;

% Set up PWL system
 setpwl([]);

a = [];
B = [];
G1 = [];
G2 = [];
```

```
F1 = [];
F2 = [];
F3 = [];
F4 = [];

dyn1 = addynamics(A1, a, B, G1);
dyn2 = addynamics(A2, a, B, G2);
dyn3 = addynamics(A3, a, B, G1);
dyn4 = addynamics(A4, a, B, G2);

% adding the regions
addregion(C1, F1, dyn1);
addregion(C2, F2, dyn2);
addregion(C3, F3, dyn3);
addregion(C4, F4, dyn4);

% Extract PWL system and plots
pwlsys = getpwl;

[t, xv] = pwlsim(pwlsys, [1 2]', [0 10]); % Simulate
 plot(xv(:,1), xv(:,2),'r','Linewidth',1);
 hold on
 [t, xv] = pwlsim(pwlsys, [-1 2]', [0 10]); % Simulate
 plot(xv(:,1), xv(:,2),'b','Linewidth',1);
 hold on
 [t, xv] = pwlsim(pwlsys, [-1 -2]', [0 10]); % Simulate
 plot(xv(:,1), xv(:,2),'y','Linewidth',1);
 hold on
 [t, xv] = pwlsim(pwlsys, [1 -2]', [0 10]); % Simulate
 plot(xv(:,1), xv(:,2),'k','Linewidth',1);
 hold on
 plot([-4 4],[0 0],'--k');
 hold on
 plot ([0 0],[5 -5],'--k');

 xlim([-4 4]);
 ylim([-5 5])

 grid on
 hold off
```